Available online at www.CivileJournal.org

Civil Engineering Journal

(E-ISSN: 2476-3055; ISSN: 2676-6957)

Vol. 11, No. 10, October, 2025

Climate Change Impacts on Rainfall Variability and Adaptive Reservoir Operation in a Multi-Reservoir System

Alexander Leda [1*], Rita Tahir Lopa [1], Farouk Maricar [1], Riswal Karamma [1*]

[1] *Department of Civil Engineering, Hasanuddin University, South Sulawesi 91711, Indonesia.*

Received 08 July 2025; Revised 22 September 2025; Accepted 27 September 2025; Published 01 October 2025

Abstract

Changes in rainfall patterns driven by climate change have altered the hydrological regime of river basins, creating substantial challenges for water resources management, particularly in the operation of the Batutegi cascade system comprising the Batutegi Dam, Way Sekampung Dam, Argoguroh Weir, Margatiga Dam and Jabung Weir. This study assesses the impacts of climate change on rainfall intensity, dependable flow, and water allocation modeling within the Sekampung River Basin. The analysis employed five rainfall datasets downscaled from the NASA Earth Exchange Downscaled Climate Projections at 30 arc-seconds (NEX-DCP30) and simulated using five CMIP6 models for both the historical period (1980–2014) and future projections (2024–2100). Results indicate that CMIP6 projections reproduce rainfall patterns reasonably well during January–February and May–July, but perform less consistently in March–April and October–November. Most models tend to overestimate the mean annual rainfall. Rainfall variability contributes to pronounced fluctuations in river discharge, particularly during the dry season. Dependable flows show marked changes, especially within the exceedance probability range of Q10% to Q100%. Although an overall increasing rainfall trend is observed, the system is still able to satisfy water demand under the 2023 operating rules, with potential deficits persisting during critical periods. Optimization modeling further demonstrates the necessity of adaptive reservoir operation rules under climate change, which could improve the reliability of meeting multisectoral demands to approximately 80%. These findings underscore the importance of incorporating climate model projections into watershed-based water resources management to strengthen resilience against extreme hydroclimatic variability.

Keywords: Climate Change; CMIP6; Rainfall Intensity; Dependable Flow; Operational Patterns.

1. Introduction

The Sekampung River Basin (DAS Sekampung) in Lampung Province, Sumatra, plays a crucial role in supporting Indonesia's food security, as the province ranks among the nation's primary rice-producing areas. The basin is traversed by the Way Sekampung River, which supports extensive water resources infrastructure, most notably the Batutegi Cascade Dam System. This system, comprising the Batutegi Dam, Way Sekampung Dam, Argoguroh Weir, Margatiga Dam, and Jabung Weir regulates and allocates water for the 89,295 ha Sekampung irrigation scheme, while also providing a raw water supply and generating hydropower (Figure 1).

Climate change is one of the major global challenges with widespread impacts on various aspects of human life and natural ecosystems. According to the Intergovernmental Panel on Climate Change (IPCC), the global average temperature has increased by approximately 1.1°C since the pre-industrial era, primarily due to rising concentrations of greenhouse gases in the atmosphere [1]. These changes affect not only temperature but also rainfall patterns, the

* Corresponding author: alexander.leda68@gmail.com; riswalk@unhas.ac.id

http://dx.doi.org/10.28991/CEJ-2025-011-10-08

frequency of extreme weather events, and the balance of the hydrological cycle in many regions of the world, including Indonesia. The impacts include more intense rainfall, higher maximum precipitation, and prolonged dry seasons, all of which threaten the reliability of water availability.

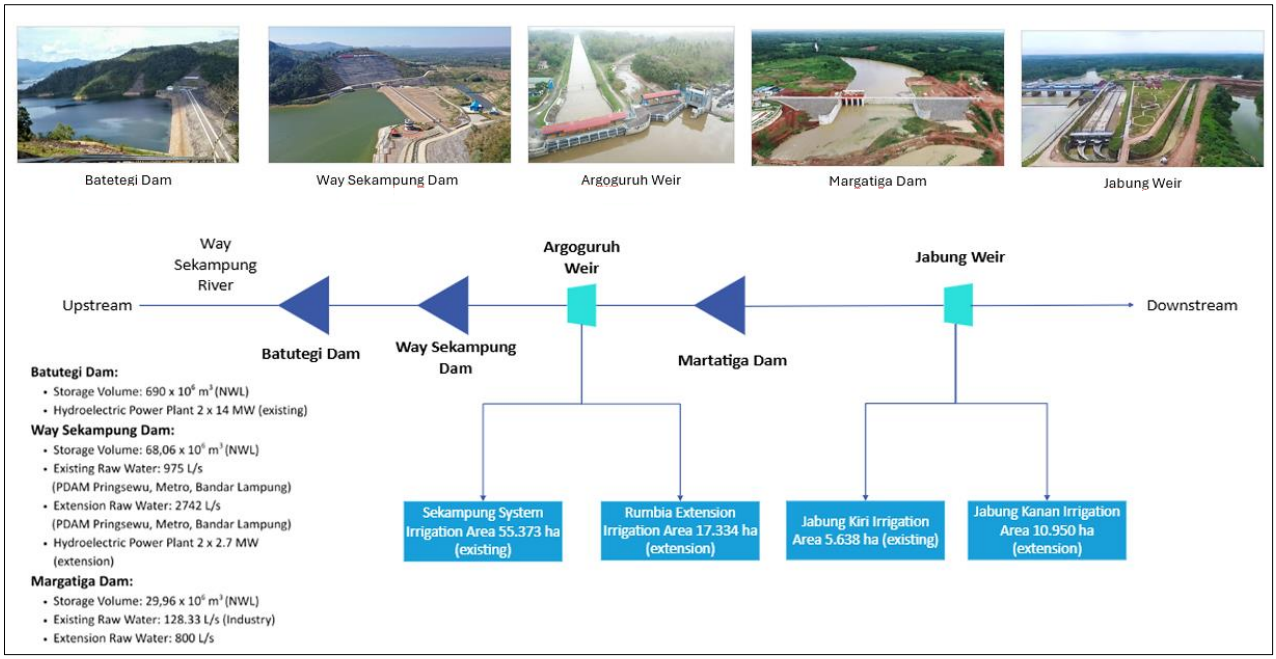

Figure 1. Way Sekampung Cascade Reservoir Scheme System

Changes in rainfall patterns across tropical regions have been extensively studied in the context of climate change [2], with direct implications for basin-scale hydrology, particularly water availability. Driven by rising temperatures and greater evaporation, rainfall patterns near the equator display more rapid and pronounced variability throughout the year [3]. This has serious consequences for irrigation-dependent areas, where both the volume and timing of water are disrupted, resulting in reduced agricultural productivity. The vulnerability of water resource systems remains high, even in regions supported by extensive infrastructure. For instance, the Sekampung irrigation system continues to face recurring difficulties in meeting water demands, often leading to crop failures [4]. The impacts of climate change are becoming increasingly evident, with more areas experiencing both droughts and floods [5].

There are only two cascade infrastructure systems of this kind in Indonesia, namely the Saguling (1986)–Cirata (1988)–Jatiluhur (1967) cascade in western Java, which has been in operation for a long time. Numerous scientific studies and publications have examined this system. In contrast, the Batutegi Cascade Infrastructure System in Lampung Province, Sumatra, was only recently developed and has been in operation since 2004 to 2024. Consequently, there is still limited literature and research on water availability and operational patterns in relation to climate change. The Batutegi Cascade System, comprising three dams and two weirs, presents more complex challenges due to its involvement with multiple stakeholders and increasing pressure from climate change. This study evaluates the impact of climate change on rainfall intensity, dependable flow, and water allocation modeling in the Sekampung River Basin (DAS). The results are used to review existing operational patterns and to develop optimal patterns that respond to current needs while adapting to future climate conditions. This research is particularly important because it is the first conducted in this region, introduces new insights using the latest CMIP6 climate models, and provides inputs for formulating government policies on adaptive and responsive water resource management in Lampung Province and Indonesia.

Previous research has shown that to obtain CMIP6 prediction values at a sub-regional scale using 31 CMIP6 models, estimates of winter and summer precipitation in the United States recommend downscaling prior to analysis, as the raw values are too generalized [6]. To predict future changes in discharge, we analyzed runoff based on projected rainfall data. We employed NASA Earth Exchange Downscaled Climate Projections at 30 arc-seconds (NEX-DCP30), simulated using five Coupled Model Intercomparison Project Phase 6 (CMIP6) climate models: MPI-ESM2-LR, MPI-ESM2-HR, MIROC6, CanESM5, and CESM2. Four scenarios were applied to each model, namely SSP12, SSP245, SSP370, and SSP585. Synthetic discharge generation was performed using the Hydrologic Engineering Center–Hydrologic Modeling System (HEC-HMS), while the River Basin Simulation Model (RIBASIM) was used to integrate HEC-HMS outputs and evaluate the system's capacity to meet water demand through 2100. In managing a multi-reservoir system such as the Sekampung River Basin, we conducted reservoir operation simulations and optimization to assess efficiency and effectiveness in meeting irrigation, domestic, and industrial water needs.

2. Theoretical Foundation

The Sekampung River Basin (DAS) is located on the island of Sumatra, Indonesia, between 104º30′34″–104º49′14″ E and 05º05′50″–05º16′33″ S. The basin covers an area of 5,675 km² and encompasses seven districts in Lampung Province Tanggamus, Pringsewu, Pesawaran, West Lampung, Central Lampung, South Lampung, and East Lampung as well as two cities, Bandar Lampung and Metro. The Way Sekampung River originates from Mount Ridingan, extends for 265 km, and comprises 62 sub-watersheds. The basin is predominantly flat, although the upper reaches have steeper slopes. Approximately 80% of the area has a gentle slope ranging from 0% to 8%, while about 2.5% has slopes greater than 40%.

Climate change, primarily driven by anthropogenic greenhouse gas emissions, has altered rainfall intensity and patterns, thereby disrupting hydrological cycles [7]. These shifts have direct implications for water availability, flood risk, and ecosystem stability. The Sekampung River Basin, a key basin in Lampung Province, is particularly vulnerable due to both climatic and anthropogenic pressures. Land cover change over the past two decades has altered flow regimes, while projections for Southeast Asia suggest an increase in rainfall intensity that could exacerbate flooding and erosion risks [8, 9].

To evaluate future scenarios, climate projections from five CMIP6 models were analyzed under four Shared Socioeconomic Pathways (SSPs) [10]. SSP1 ("Sustainability") represents a cooperative, low-emission pathway with sustainable growth and equitable development. SSP2 ("Middle of the Road") depicts moderate transitions in energy, population, and economic growth, with partial progress toward climate goals. SSP3 ("Regional Rivalry") illustrates fragmented development with high population growth, limited cooperation, and widening inequality. Together, these SSPs provide a framework for assessing potential hydrological impacts on the Sekampung River Basin under contrasting socio-economic and climate futures (Figure 2).

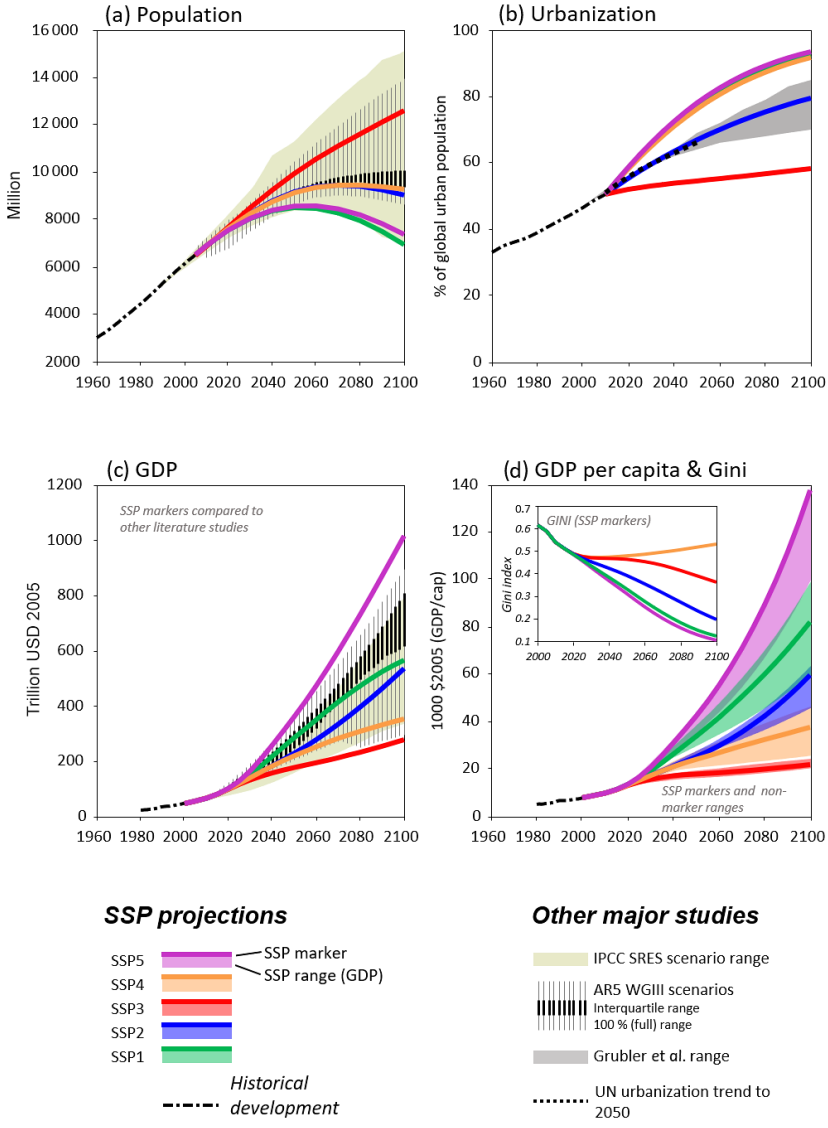

Figure 2. Socioeconomic assumptions associated with each SSP, including population, urbanization, and GDP

Shared Socioeconomic Pathway 4 (SSP4), commonly referred to as the "Inequality" scenario, describes a world characterized by pronounced disparities in wealth distribution, where economic gains concentrate among the affluent while disadvantaged groups are left behind. Population growth is unevenly distributed, often leading to unplanned urbanization, social stress, and environmental degradation. Economic expansion under this pathway is concentrated in high-income countries, with rising per capita GDP in wealthier regions, while developing nations struggle to achieve comparable growth. The high Gini index associated with SSP4 reflects a deepening of inequality and persistent socioeconomic challenges.

Both SSP3 and SSP4 are marked by energy systems that remain heavily reliant on coal, resulting in elevated greenhouse gas (GHG) emissions due to limited access to renewable energy sources. Weak institutional performance, ineffective land-use policies, and inconsistent regional regulations on air pollution and GHG mitigation further exacerbate environmental degradation [11, 12]. These scenarios are often associated with high pollutant and aerosol emissions, contributing to adverse climate outcomes.

The simulations were conducted using five climate models: Max Planck Institute version 2 Low Resolution (MPI2LR), Max Planck Institute version 2 High Resolution (MPI2HR), Model for Interdisciplinary Research on Climate version 6 (MIROC6), Canadian Earth System Model version 5 (CanESM5), and Community Earth System Model version 2 (CESM2). MPI2LR, developed by the Max Planck Institute for Meteorology in Germany, provides a crucial foundation for assessing the effects of climate change on key sectors, including agriculture, water resources, and public health, and informs the development of mitigation policies. MPI2HR is similar in design but offers higher spatial resolution. MIROC6 enables the study of climate change processes and the identification of potential extreme weather patterns. CanESM5 simulates climate change and its impacts by considering complex interactions among the atmosphere, oceans, ice, and biosphere. CESM2, developed under the leadership of the University Corporation for Atmospheric Research (UCAR) with contributions from global institutions, is part of the Community *Earth System Model* and provides a widely used framework for climate system research.

Global climate change alters rainfall and temperature patterns, directly affecting the availability and variability of water resources in river basins. These fluctuations increase uncertainty in water management, particularly in irrigation and reservoir systems dependent on river discharge [13, 14]. In the Sekampung River Basin, rainfall changes under different climate scenarios may shift flow patterns at both seasonal and annual scales, with implications for raw water supply, agriculture, and hydropower generation. To assess river discharge dynamics under such conditions, hydrological models such as the Hydrologic Engineering Center–Hydrologic Modeling System (HEC-HMS) are applied. HEC-HMS converts rainfall data into discharge (rainfall–runoff modeling) and is widely used to evaluate watershed responses to different climate scenarios [15, 16]. Model calibration and validation were conducted using historical data (1980–2023), and the validated models were then applied for projections (2024–2100).

In multi-reservoir water management systems, such as the Sekampung River Basin, reservoir operation simulations are crucial for assessing efficiency in meeting irrigation, domestic, and energy demands. Reservoir optimization utilizes dynamic programming to determine optimal water release decisions, taking into account inflow volume, storage capacity, downstream requirements, and hydropower production [17]. The height–volume–area (H–V–A) curve was used as a constraint in developing adaptive operation strategies.

The River Basin Simulation Model (RIBASIM) is a decision-support tool for watershed-level water management. It represents both physical systems (rivers, reservoirs, channels) and management systems (demands, allocation priorities), enabling the simulation and optimization of water balances under various supply and demand scenarios [18]. In this study, RIBASIM was used to integrate HEC-HMS simulation results and evaluate the capacity of the Sekampung system to meet water demand until 2100, as well as to assess water allocation strategies at the basin scale [19].

3. Research Methodology

3.1. Rainfall Intensity Analysis

The analysis of the impact of climate change on rainfall intensity consists of several stages, including the collection of CMIP6 climate model projection data and ground station data, as well as the analysis of future rainfall intensity.

3.2. CMIP6 Climate Model Collection

The CMIP6 climate projection models, which have a native spatial resolution of 1 ° × 1 ° (approximately 4,136.8 km² in the Sekampung watershed), are too coarse to accurately represent local hydrological characteristics. Therefore, bias correction of CMIP6 rainfall outputs was performed using ground-based observations. The rainfall data preparation consisted of three main components:

- Downscaled climate data, obtained from the NASA Earth Exchange Downscaled Climate Projections (NEX-DCP30) at 30-arc second (~1 km) resolution, specifically daily rainfall;
- Climate models, including five CMIP6 GCMs (MPI2LR, MPI2HR, Miroc6, CanESM5, and CESM2), with a historical baseline (1981–2014) and future projections (2024–2100) under four SSP scenarios (SSP1-2.6, SSP2-4.5, SSP3-7.0, SSP5-8.5);

- Ground observations, comprising daily rainfall data from 212 rain gauge stations (1981–2023) provided by the Mesuji–Sekampung River Basin Agency (BBWS).

From these stations, only gauges with continuous records exceeding 30 years and less than 5% missing data were retained. Missing values were estimated using weighted averages from the nearest stations. Data consistency was verified through double mass curve analysis, ensuring long-term reliability and accuracy. Regional rainfall was then calculated using the Thiessen polygon method in ArcGIS Pro (Equation 1).

$$d = \frac{\sum A_i.P_i}{A} \quad (1)$$

where d is the rainfall in the region, A is the area, A_i is the area affected by rainfall stations 1, 2, 3, ..., n, and P_i is the rainfall at rainfall stations 1, 2, 3, ..., n.

3.3. Verification of CMIP6 Climate Projection Data Models

The validity of the CMIP6 daily rainfall projections was evaluated by comparing simulated values with ground-based observations for the historical period (1980–2014). This validation step aimed to determine the models' ability to reproduce observed rainfall characteristics in the study area before applying them to future projections (2024–2100). The verification procedure consisted of four components:

- Visual comparison of seasonal rainfall patterns between observations and projections;
- Comparison of monthly mean rainfall values;
- Comparison of annual mean rainfall values; and
- Statistical evaluation using the Root Mean Square Error (RMSE).

RMSE was used to quantify the average difference between projected and observed rainfall. It was calculated as:

$$RMSE = \sqrt{\frac{1}{|n|}\sum_{i=1}(Obs_i - Pred_i)^2} \quad (2)$$

where n is Number of observations, *Obs* is observed rainfall value, and *Pred* is Predicted rainfall value.

3.4. Rainfall Trend Analysis

Trends in extreme rainfall events were assessed using climate indices recommended by the World Meteorological Organization (WMO) [20]. The indices applied in this study include:

- **Consecutive Dry Days (CDD):** the maximum number of consecutive days with daily rainfall less than 1 mm.
- **Consecutive Wet Days (CWD):** the maximum number of consecutive days with daily rainfall equal to or greater than 1 mm.
- **Rx1Day:** the highest single-day rainfall recorded within a specified period.
- **Rx5Day:** the highest cumulative rainfall over any consecutive five-day period.
- **PRCPTOT:** the total precipitation accumulated over a specified period.

These indices were calculated from daily rainfall data to quantify the frequency and intensity of extreme precipitation events in the study area.

3.5. Dependable Flow

The estimation of dependable flow required multiple datasets, including hydrological, topographic, land use, and soil data. Hydrological inputs comprised rainfall data from five CMIP6 climate models under four Shared Socioeconomic Pathway (SSP) scenarios, ground-based rainfall observations, and discharge records from Automatic Water Level Recorder (AWLR) stations located at several river sites. Topographic information was obtained from the Digital Elevation Model (DEM) provided by the Geospatial Information Agency (BIG), while land use and soil data were sourced from the Ministry of Environment and Forestry and the Food and Agriculture Organization (FAO).

The operation of the Batutegi Cascade Dam System largely depends on the availability of river flow. However, discharge records managed by the Mesuji–Sekampung River Basin Agency (BBWS) are temporally discontinuous and unevenly distributed across the watershed. To overcome these limitations, synthetic daily discharge was generated using

observed rainfall data for historical conditions and satellite-based rainfall projections from CMIP6 models for future scenarios (1980–2100).

Rainfall–runoff transformation was simulated using the Hydrologic Engineering Center – Hydrologic Modeling System (HEC-HMS). Required model inputs included rainfall, land use, soil type, and topography. The watershed was subdivided into smaller sub-catchments to better represent spatial heterogeneity. The modeling framework consisted of: (i) watershed delineation, (ii) identification of rainfall and discharge stations for input and calibration, (iii) model development, (iv) calibration using observed discharge, (v) generation of daily discharge from ground rainfall records, and (vi) projection of discharge under CMIP6 climate scenarios.

Model performance was evaluated by comparing simulated and observed discharges. Two statistical indicators were employed: Nash–Sutcliffe Efficiency (NSE), which measures model accuracy, and Percent Bias (PBIAS), which quantifies systematic deviations (Table 1). These indices are widely used in hydrological modeling to assess goodness of fit [21, 22].

Table 1. Recommended Performance Rating

No.	Goodness of Fit	NSE	PBIAS
1	*Very good*	E>0.6	PBIAS<±10
2	*Good*	0.4<E≤0.6	±10≤ΠBIAΣ≤±15
3	*Satisfactory*	0.2<E≤0.4	±15≤ΠBIAΣ≤±25
4	*Unsatisfactory*	E<0.2	PBIAS>±25

Dependable flow analysis was conducted to support the calculation of reservoir operation patterns, thereby providing managers with a more measurable basis for future planning. The analysis focused on determining discharges at the 80%, 90%, and 95% probability levels, which represent the flow rates expected to be equaled or exceeded at the specified probabilities. The calculation followed the procedure outlined in the Indonesian National Standard (SNI) No. 19-6738-2015, as presented in Equation 3.

$$P(X \geq x) = \frac{m}{n+1} \times 100\% \quad (3)$$

where $P(X>x)$ is The probability that the discharge variable X exceeds a threshold of x m³/s., m is rank order of the discharge value, n is total number of discharge data points, X is discharge time series and x is dependable flow if the probability matches its intended use.

3.6. Optimization of the Batutegi Cascade Reservoir Operation Pattern System

The operational pattern of the Batutegi Cascade Reservoir System was optimized to ensure adequate water supply for downstream sectors, including agriculture, irrigation, industry, and domestic use, while maintaining the balance between inflow and outflow. The optimization process was conducted to promote efficient water use and ensure availability, particularly for irrigation and community needs.

The sustainability of infrastructure, river systems, human activities, and ecosystems is strongly influenced by regional climatic conditions. Extreme events, such as floods and droughts, disrupt the continuity of water supplies for irrigation, domestic use, and hydropower generation [23, 24]. Variations in hydroclimatological parameters due to climate change directly affect reservoir operations, mainly through changes in rainfall and temperature [6], which alter evapotranspiration and water availability within the catchment area [25]. According to the Intergovernmental Panel on Climate Change (IPCC), the average temperature in Indonesia has increased by approximately 0.3%, while annual rainfall has declined by 2–3%, particularly in the southern region [26–28]. These changes influence reservoir inflow and necessitate adaptive operational strategies.

Optimization in this study was applied as a mathematical approach to determine optimal solutions under given constraints [29]. This approach addresses resource limitations by maximizing benefits and minimizing negative impacts, and it is considered an essential tool for supporting the long-term sustainability of water resources [30].

3.6.1. Reservoir Simulation

Reservoir simulations were conducted to plan and manage water storage, flow, and utilization in accordance with demand and availability. In this study, the baseline calibration of climate change impacts on rainfall was carried out for the period 1980–2014. Rainfall–runoff transformation into discharge was performed using the open-source

Hydrologic Engineering Center–Hydrologic Modeling System (HEC-HMS). The model was calibrated for discharge using Automatic Water Level Recorder (AWLR) data from four river locations between 2014 and 2016, and subsequently verified with rainfall data from 2009 to 2023. To integrate the HEC-HMS results and evaluate system capacity, the open-source River Basin Simulation Model (RIBASIM) was applied. Water availability simulations were combined with water allocation patterns based on the Water Resources Management Plan (WRMP) for the Sekampung river basin, with 2023 as the base year. All simulations were performed using a half-monthly time step for the period from 1980 to 2023.

Figure 3 illustrates the timeline of the calibration and validation processes for the various components of the integrated water allocation model. This step is crucial to ensure the model's reliability for future scenario projections and to support decision-making in water resource management. Reservoir simulation projections were conducted for the designated projection period, as reflected in the modeling framework and depicted in Figure 3.

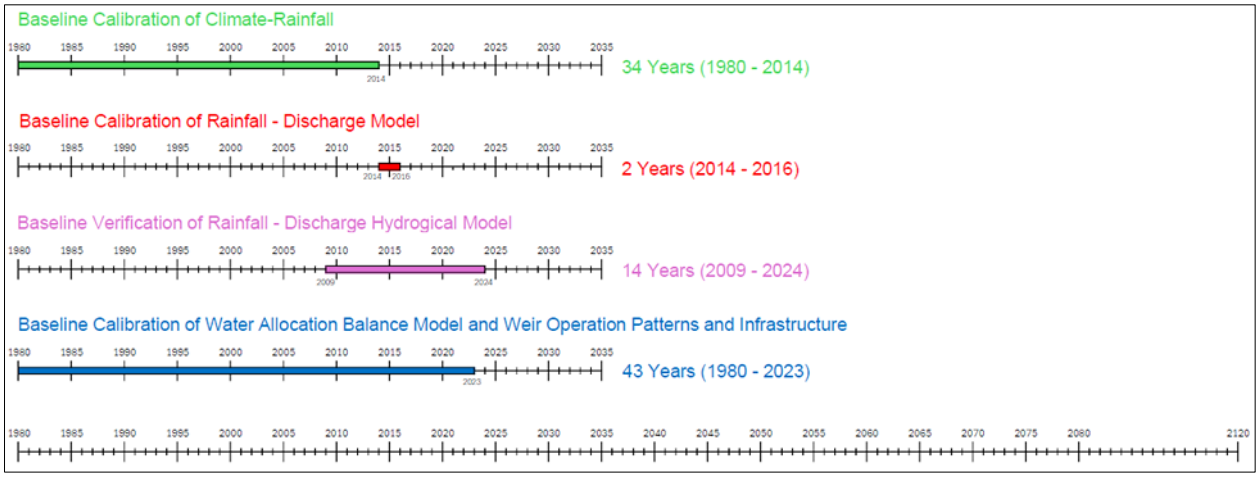

Figure 3. Time period of projection in modeling

3.6.2. Reservoir Simulation Projections for each Scenario

Water availability projections for the period 2024–2100 were generated using HEC-HMS with calibration parameters from 2014 to 2016, under the assumption that no parameter changes occurred during the projection period. The projected discharge was then used to simulate the operation of the Batutegi Cascade Reservoir System, assuming that infrastructure conditions and operational patterns remain consistent with those outlined in the 2023 Natural Resources Development Plan.

3.6.3. Reservoir Operation Optimization

Reservoir operation optimization was conducted using dynamic programming to determine the optimal outflow release based on inflow conditions. The optimization process incorporated height–volume–area (H–V–A) curve constraints, electricity production targets, structural limitations, and downstream water demand. Reservoir operations were then represented as water level variations and plotted on a single graph using the same annual time range for each reservoir.

3.6.4. Optimization of Water Allocation Balance Model Calibration (Period 1980-2023)

The calibration of the Water Balance–Allocation Model for the Batutegi Cascade Reservoir System in RIBASIM (1980–2023) was based on input data of reservoir operation patterns and existing dam infrastructure as of 2023. The model incorporated river flow inputs from gauging stations derived from HEC-HMS simulations for the 1980–2023 dataset, applying a semi-monthly time step to capture operational dynamics. Reservoir outflow optimization was performed using a dynamic programming approach, with system constraints including inflow rates, area–volume relationships, power generation targets, and downstream water demands.

3.6.5. Water Allocation Balance Projection (2024-2100)

The water allocation balance projection was conducted under the assumption that the 1980–2023 period represents existing conditions, including reservoir and infrastructure operation patterns, as well as supply–demand conditions, in accordance with the 2023 Natural Resources Development Plan of the Mesuji–Sekampung River Basin Management Agency. To assess the patterns of fulfilment under climate change (2024–2100), simulations were conducted using the existing reservoir operation scheme with predicted inflow discharge derived from climate change models.

3.7. Research Implementation

This study evaluates the impact of climate change on rainfall intensity, dependable flow, and water allocation in the Way Sekampung River Basin (DAS). The analysis employed five sets of rainfall data scaled from the NASA Earth Exchange Downscaled Climate Projections (NEX-DCP30) with a spatial resolution of 30 arc seconds. Simulations were conducted using five climate models from the CMIP6 scheme, encompassing both the historical period (1980–2014) and future projections (2024–2100). Dependable flow estimates were then used to develop and optimize reservoir operation patterns that are adaptive to future climate change. The findings of this study provide technical recommendations for stakeholders and policymakers, particularly in the field of water resources management.

3.8. Research Visualization Sketch

A research process flowchart illustrates the sequence of stages undertaken in this study, providing a clear overview of the workflow from the initial stage to the final stage. The flowchart is presented in Figure 4.

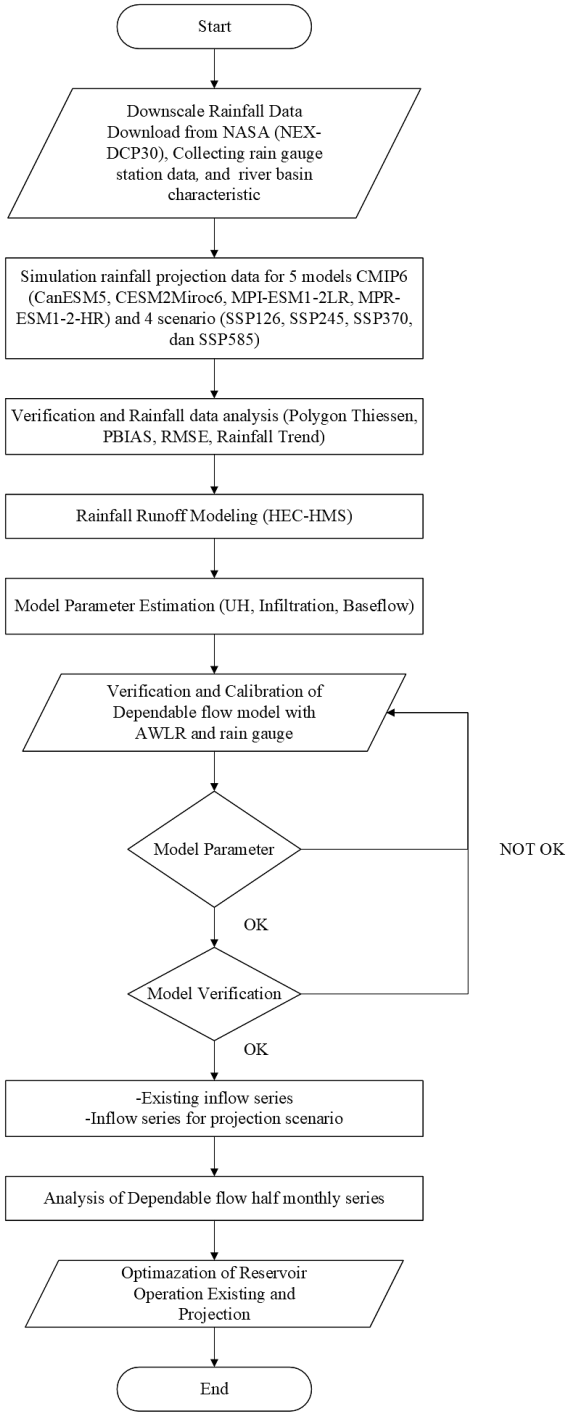

Figure 4. Research Process Flowchart

4. Results and Discussion

4.1. Download Data (1950-2100)

4.1.1. CMIP6 Climate Model Collection

The Coupled Model Inter-comparison Project Phase 6 (CMIP6) [31] is among the latest climate modeling frameworks and has shown notable improvements compared to its predecessor (CMIP5), particularly in spatial resolution and the representation of cloud microphysics [6]. Despite these advancements, the application of CMIP6 simulations in the Indonesian region remains limited, which poses challenges for localized hydrological assessments. Accurate rainfall and temperature projections are critical, as they directly influence the determination of Reservoir Operation Patterns (ROP). However, the relatively small spatial coverage of the study area (4,136.8 km²) highlights a key limitation. The coarse resolution of the CMIP6 outputs (1° × 1°) [32] cannot adequately represent the heterogeneity of watershed characteristics. To overcome this issue, the NASA Earth Exchange Downscaled Climate Projections (NEX-DCP30) [33] were applied, providing daily rainfall data at a higher resolution (30 arc seconds). Four Shared Socioeconomic Pathway (SSP) scenarios—SSP1-2.6, SSP2-4.5, SSP3-7.0, and SSP5-8.5—were analyzed. The use of five NEX-DCP30 datasets allowed for the assessment of rainfall variability during the historical period (1981–2023) and the projection period (2024–2100) across an 8 × 8 grid. The results emphasize that downscaling is essential for capturing localized rainfall dynamics, which cannot be represented adequately by the coarse-resolution CMIP6 datasets. This adjustment ensures a more robust analysis of rainfall changes, providing a stronger basis for subsequent hydrological modeling and reservoir operation strategies in the Sekampung River Basin.

4.1.1. Verification of CMIP6 Climate Projection Data Models

This study utilizes observed daily rainfall data to calibrate a reduced dataset in the Sekampung river basin area. The data was obtained directly from the Mesuji-Sekampung River Basin Agency (BBWS). There are 212 rainfall stations; however, this study utilizes data from a subset of selected measuring stations that consistently cover the period from 1980 to 2023. For quality control, we reconstructed the dataset by selecting only stations with more than 30 years of observations and less than 5% missing data. To address data gaps, missing data were filled in using the weighted average of the nearest neighboring stations. Additionally, a double mass curve analysis was applied to compare each station with its nearest neighbors, ensuring a reliable and continuous time series reconstruction. Rainfall stations are mostly concentrated in flat areas with slopes of less than 8%, covering more than 56% of the river basin. This spatial limitation contributes to uneven rainfall coverage, limiting the ability to accurately capture local rainfall patterns in the region. Therefore, we distributed the weights of each gauge using Thiessen polygons with ArcGIS Pro software. Of the 212 rainfall measuring stations at the location, only 39 (18.4%) were selected, indicating that 81.6% of the data from the rainfall stations in the Sekampung river basin were not well-documented. The results of the Thiessen polygon method, as calculated using ArcGIS Pro software, are presented in Table 2.

Table 2. Thiessen polygon weights for ground rainfall stations

No.	Rainfall Station	Area (km^2)	Weights Poligon Thiessen
1	Air Naningan	444.09	10.74%
2	Banjar Agung	118.55	2.87%
3	Banyuwangi	30.13	0.73%
4	Batu Keting	67.72	1.64%
5	Bendung Argoguruh	108.23	2.62%
6	Bulok	100.02	2.42%
7	Bumi Asri Natar	87.51	2.12%
8	Bungkuk	159.88	3.86%
9	Gadingrejo	46.35	1.12%
10	Gedung Dalem	57.76	1.40%
11	Gedung Tataan	8.84	0.21%
12	Gisting Atas	111.13	2.69%
13	Gunung Batu	93.27	2.25%
14	Gunung Megang	171.11	4.14%
15	Gunung Sari	244.06	5.90%
16	Jabung	88.37	2.14%
17	K. Baru Natar	135.91	3.29%
18	Metro Barat	1.11	0.03%
19	Metro DPU	120.24	2.91%
20	Natar	108.77	2.63%
21	Pagelaran - 015	42.38	1.02%
22	Pagelaran - 018	98.48	2.38%
23	Pajaresuk	24.12	0.58%
24	Pringsewu	10.02	0.24%
25	Pajaresuk II	17.95	0.43%
26	Penengahan	72.87	1.76%
27	Pesawaran	121.77	2.94%
28	Podorejo	89.20	2.16%
29	Sekampung Udik	91.39	2.21%
30	Sukadana	271.75	6.57%
31	Sukarame	83.65	2.02%
32	Talang Baru	274.51	6.64%
33	Tanjung Bintang	279.92	6.77%
34	Trimurjo	70.57	1.71%
35	Way Gatel	47.36	1.14%
36	Way Harong	105.36	2.55%
37	Way Lima	13.98	0.34%
38	Way Semah	49.15	1.19%
39	Wonodadi	69.33	1.68%

4.2. Rainfall Data Analysis (PBIAS, RMSE, Rainfall Trends)

4.2.1. Existing Rainfall and Rainfall Projections (2015-2100) CMIP6

In Figure 5, *CanESM5* shows daily rainfall fluctuations in the range of approximately 0–60 mm/day, with a fairly consistent seasonal pattern (annual cycle) from year to year. Rainfall peaks occur periodically, indicating the model's ability to capture seasonal variability. There are a few extreme outliers exceeding 60 mm/day, suggesting that this model tends to be conservative in simulating extreme rainfall events. In Figure 6, *CESM2* displays highly variable daily rainfall patterns, with sharper and more extreme fluctuations than CanESM5. Rainfall events exceeding 80 mm/day reflect a higher intensity of extremes, and the model appears to be responsive to ENSO phenomena or global-scale climate disturbances. In Figure 7, *MIROC6* visualizes daily rainfall with more frequent peak intensities and a higher frequency of rainfall events, with intensity ranging from 0 to 100 mm/day. This model simulates more intense extreme rainfall than CanESM5 and CESM2, making it suitable for urban hydrology studies and drainage system design sensitive to peak rainfall.

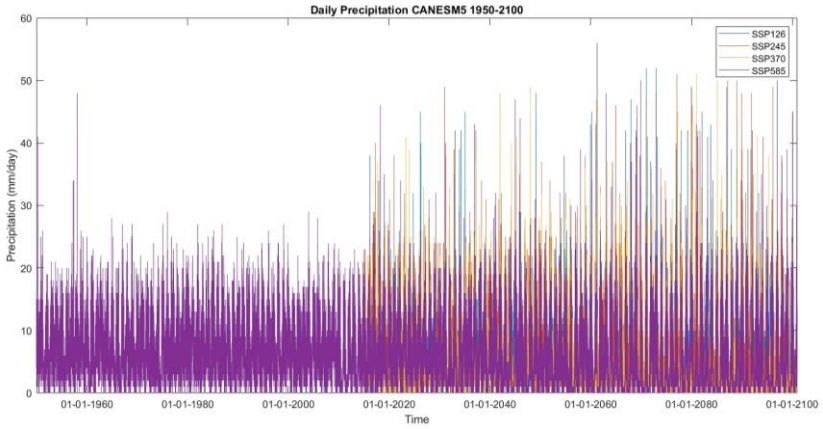

Figure 5. CanESM5 Daily rainfall projection results (1980–2014)

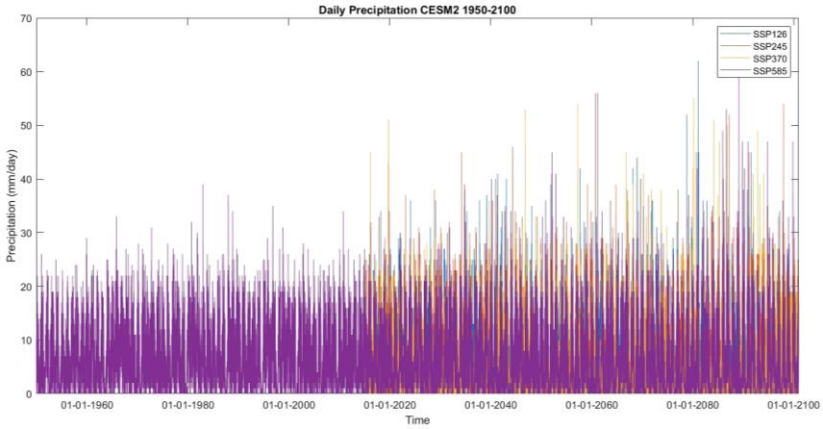

Figure 6. CESM2 Daily rainfall projection results (1980–2014)

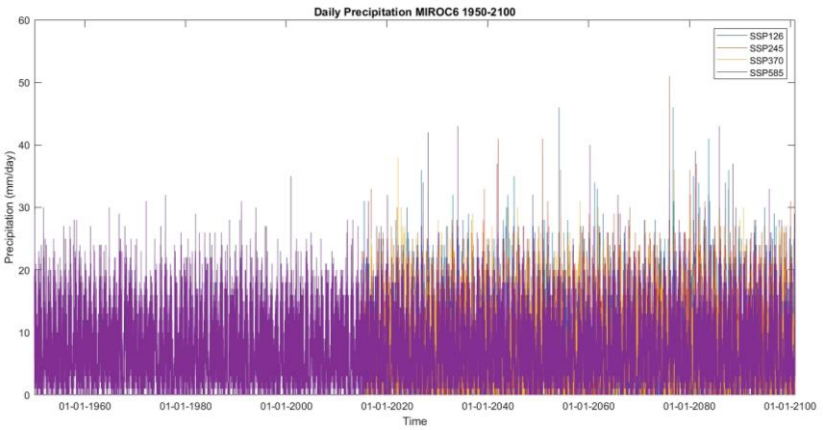

Figure 7. MIROC6 Daily rainfall projection results (1980–2014)

In Figure 8, *MPI-ESM1-2-LR* exhibits more moderate rainfall patterns, consistently reproduced from year to year within a daily intensity range of less than 80 mm/day. The model presents a stable seasonal cycle and fewer daily extremes, providing a strong baseline for long-term trend analysis. It is suitable for conservative approaches in dam design and watershed management. In Figure 9, *MPI-ESM1-2-HR* reveals sharper rainfall fluctuations and more frequent daily rainfall peaks, indicating sensitivity to local or subregional dynamics, with some events exceeding 100 mm/day. This model is well-suited for assessing flood risk and analyzing extreme events at the local scale.

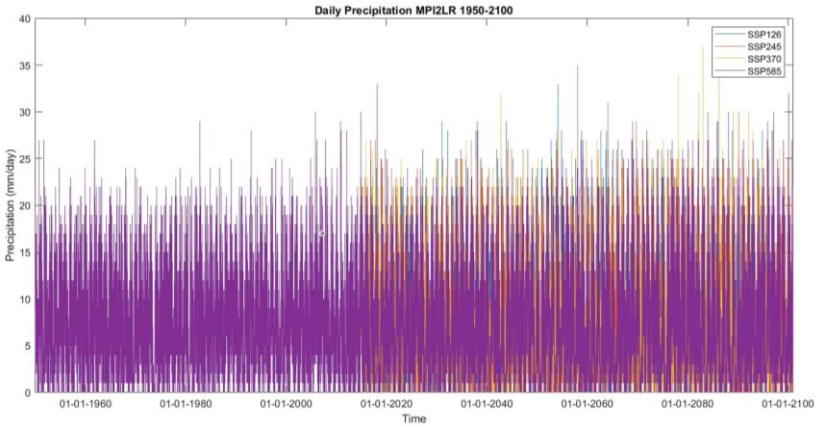

Figure 8. MPI-ESM1-2-LR Daily rainfall projection results (1980–2014)

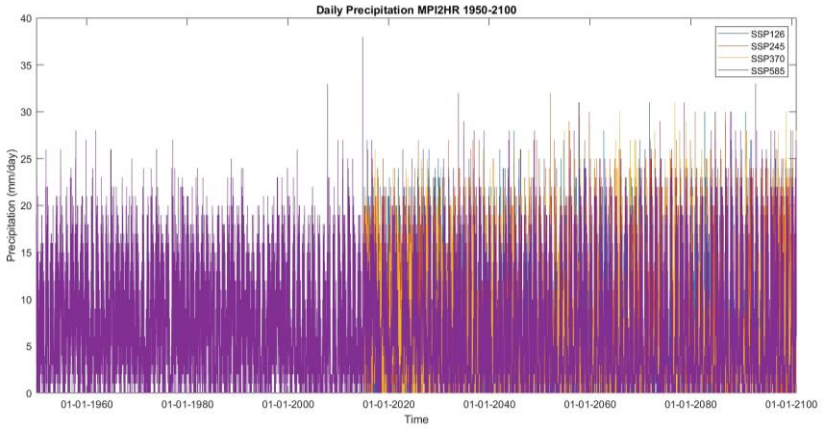

Figure 9. MPI-ESM1-2-HR Daily rainfall projection results (1980–2014)

Overall, when compared with observations from 39 ground-based rainfall stations, the bias-corrected daily rainfall outputs of the CMIP6 models for the historical period (1980–2014) show good agreement with observed data. Therefore, the projected daily rainfall data (2024–2100) from these CMIP6 models can be confidently used for future rainfall analysis and as a reference for climate impact assessments in water resource planning.

4.2.1. Comparison of Historical Rainfall and Projected Rainfall from the CMIP6 Climate Model

Rainfall from the CMIP6 model was examined in two temporal windows, namely the historical baseline (1980–2014) and the end-of-century projection (2024–2100). Historical simulations were compared with high-resolution downscaled products to evaluate consistency between datasets. Figure 10 presents the monthly average and monthly total rainfall for the Mesuji-Sekampung region. Dry months were identified based on the Köppen climate classification, which designates this region as a Tropical Rainforest Climate (Af) [34]. In this system, a month is classified as a dry month if the total rainfall is below 60 mm. Temporal distribution of downscaling products (solid lines) and gauge stations (dashed lines) for monthly average rainfall in the Mesuji-Sekampung region. The gauge station average was calculated using 35 years of data from 39 meteorological stations, and the shaded area indicates the dry season.

Daily rainfall values (Figures 11 and 12) from ground stations (x-axis) and five scaled CMIP6 model outputs (y-axis), separated by seasonal period: (rainy season) October–June and (dry season) July–September. The climate type in WS Mesuji-Sekampung is tropical rainforest (Köppen Af), characterized by two distinct seasons: the rainy season (October–June) and the dry season (July–September). From October to June, most CMIP6 model estimates tend to underestimate high-intensity rainfall events. This can be seen in the figure below, where in Figure 11 the concentration of points is denser below the 1:1 line, especially for daily rainfall totals above 20 mm.

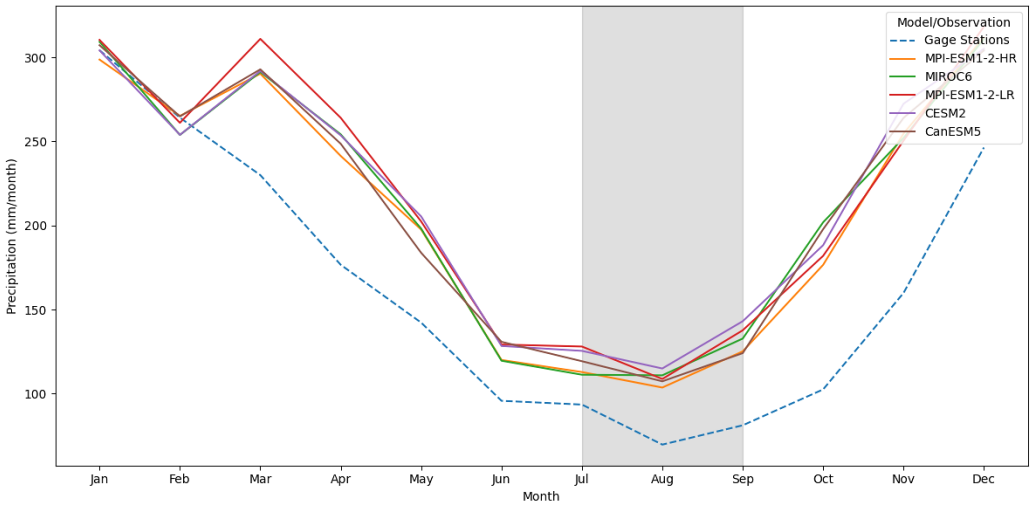

Figure 10. Monthly average rainfall in the CMIP6 region (solid line) and observations (dashed line) for Mesuji-Sekampung from 1980 to 2014

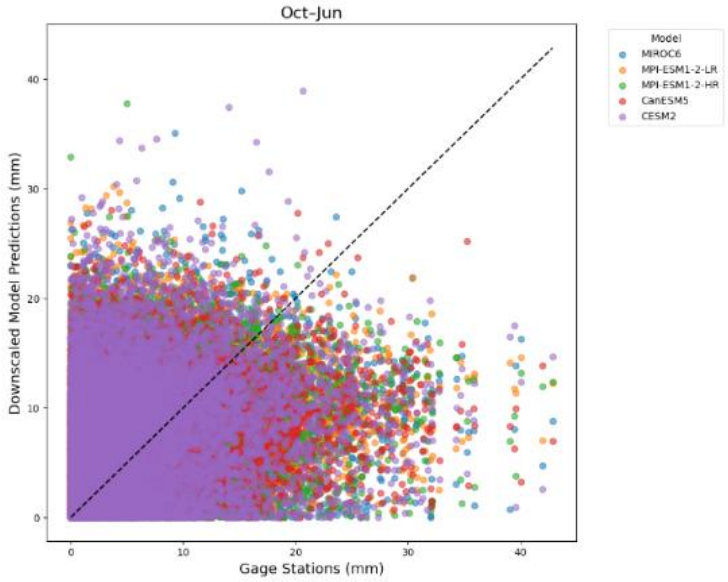

Figure 11. Daily rainfall values (Oct-Jun)

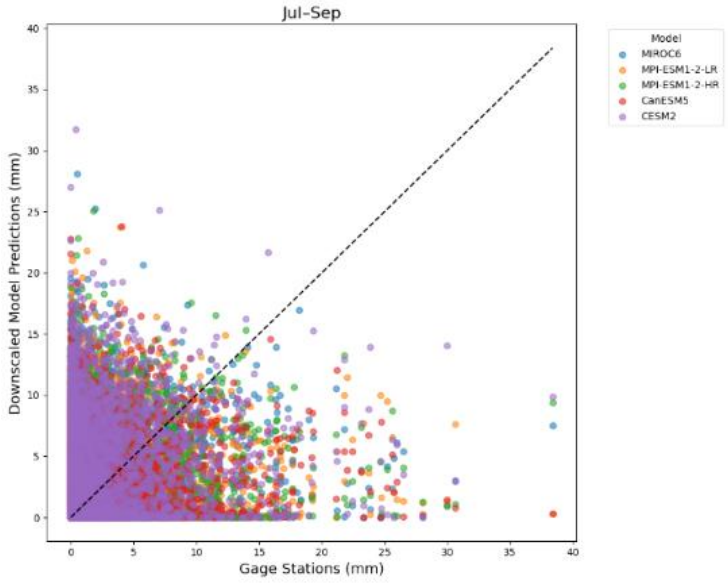

Figure 12. Daily rainfall values (Jul-Sep)

The large distribution spread indicates a fairly high bias in describing peak rainfall events (high rainfall). Therefore, it can be said that the CMIP6 model is not sufficiently accurate in describing high rainfall during the rainy season. Meanwhile, during the dry season from July to September, the distribution is smaller at low rainfall values, indicating that the CMIP6 projection model performs better in describing low rainfall during this period in the Sekampung River Basin.

Root Mean Square Error (RMSE) measures the magnitude of the difference or error between the CMIP6 projection model and observations at ground stations. The higher the RMSE value, the greater the difference between the observations and the model. The RMSE value cannot indicate whether the model underestimates or overestimates the observed values. Figure 13 shows that the RMSE value indicates that throughout the period 1980-2014, the CMIP6 projection model was able to represent the rainfall characteristics at the Mesuji-Sekampung WS very well in January, February, May, June, July, August, September, and December. It was not good enough in March, April, October, and November. In general, it is suitable for further analysis.

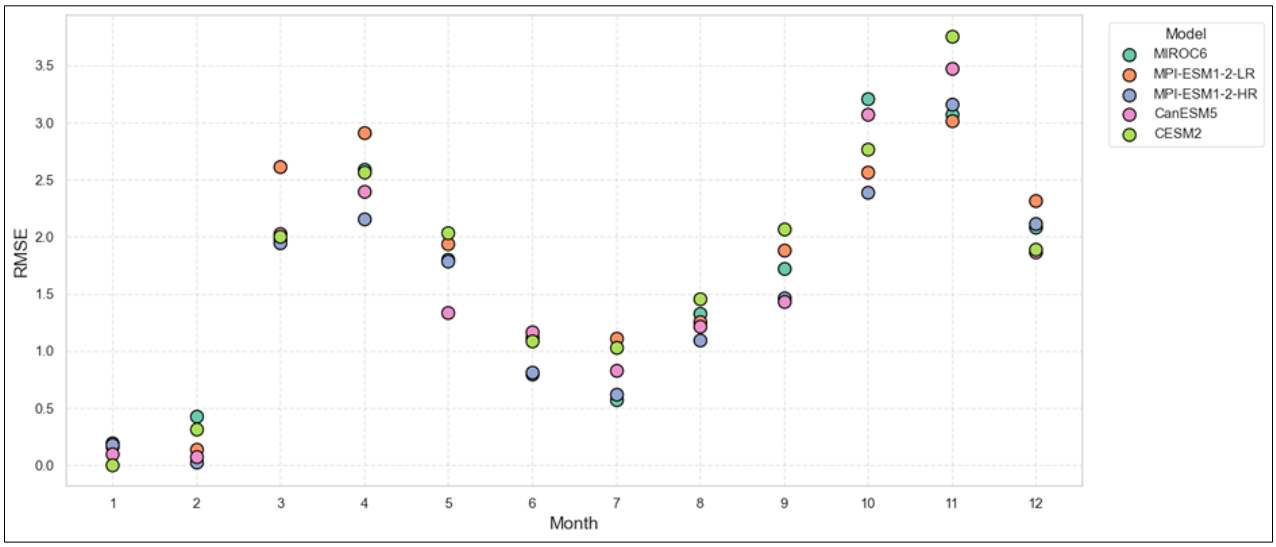

Figure 13. Average monthly RMSE between ground stations and five CMIP6 models for 1980-2014

The boxplot shown in Figure 14 illustrates the distribution of differences in annual rainfall between CMIP6 models and ground station observation datasets. Each box represents a model: MIROC6, MPI-ESM1-2-LR, MPI-ESM1-2-HR, CanESM5, and CESM2. All CMIP6 models show a positive median bias, meaning that most models tend to overestimate the observed values each year. MPI-ESM1-2-LR and CESM2 show a wider interquartile range and more extreme outliers, indicating greater interannual variability. In contrast, MIROC6, MPI-ESM1-2-HR, and CanESM5 exhibit narrower boxes, indicating that their annual differences from observed annual rainfall are more consistent over time. Although all models generally overestimate, the presence of outliers in each model indicates that model performance differs significantly from the average pattern.

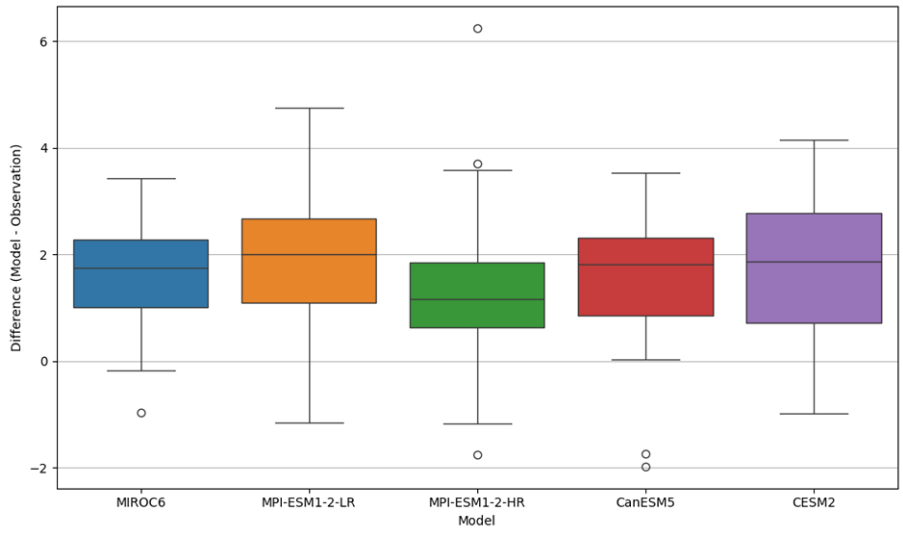

Figure 14. Average annual rainfall differences between ground stations and five corrected CMIP6 models, 1980–2014

The following figures show the differences in climate indices per year and five CMIP6 models for the period 1950-2099. Changes in rainfall characteristics at the study site from 1950 to 2099 are illustrated in five climate indices: CDD (Figure 15), CWD (Figure 16), Rx1Day (Figure 17), Rx5Day (Figure 18), and PRCPTOT (Figure 19). Each index is calculated annually. To facilitate data reading, the data is presented per decade, where the decade value is the maximum value of 10 years of data. CDD shows the number of days with the longest consecutive period without rainfall in the region, while CWD shows the number of consecutive days with rainfall. PRCPTOT indicates the annual rainfall value (Figure 16). Meanwhile, Rx1Day (Figure 17) indicates the maximum total rainfall in a single day, and Rx5Day indicates the total rainfall over five consecutive days in a year.

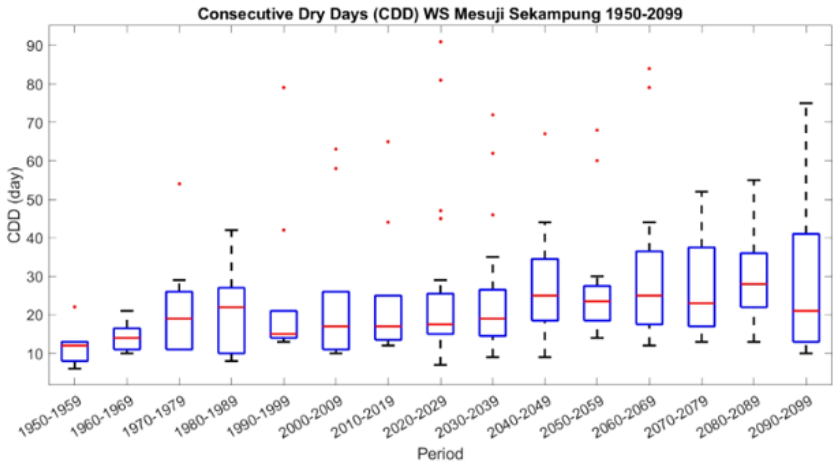

Figure 15. Climate index CDD

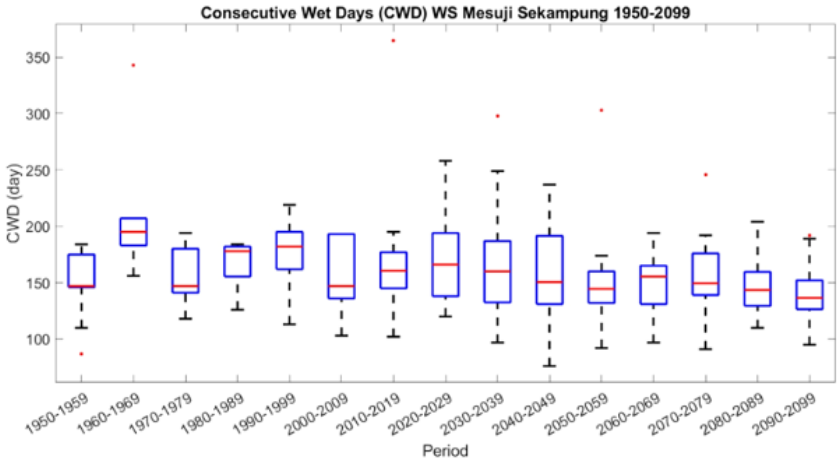

Figure 16. Climate index CWD

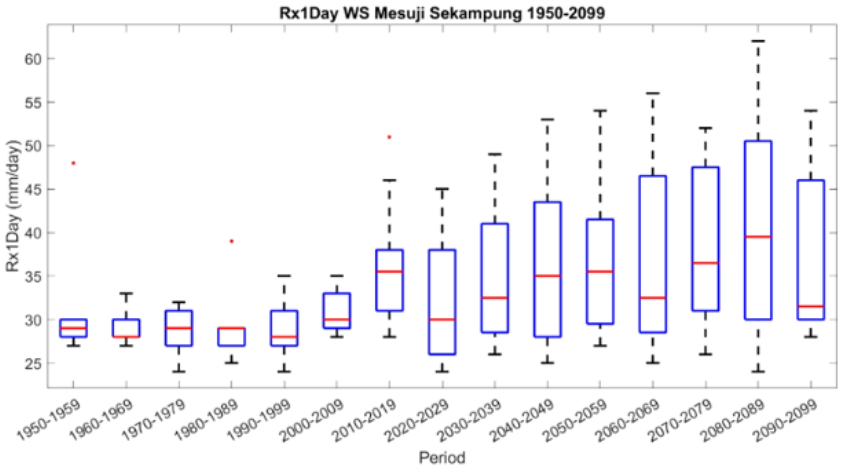

Figure 17. Climate index Rx1day

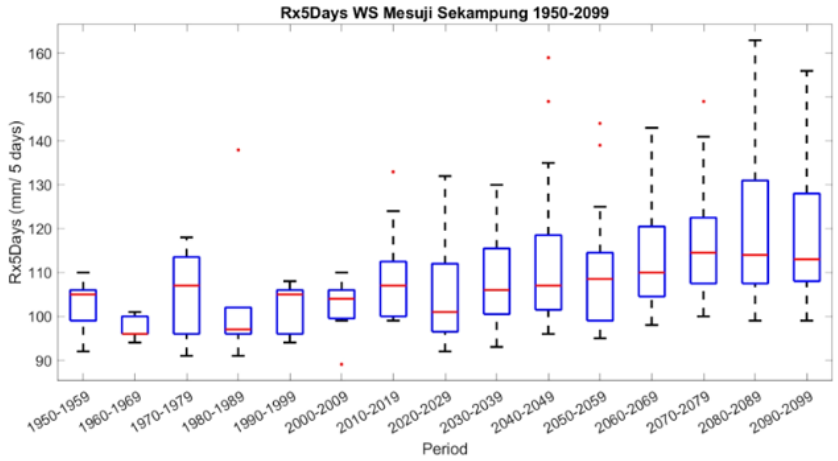

Figure 18. Climate index Rx5Day

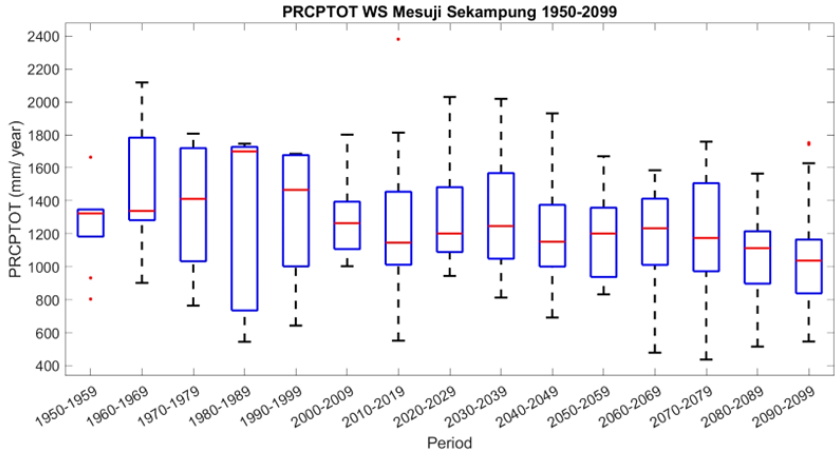

Figure 19. Climate index PRCPTOT

Based on the analysis, the CWD value (Figure 15) shows a significant downward trend, decreasing by 28 days over 150 years (equivalent to 7 days every 30 years) in consecutive rainy days. Conversely, the CDD value (Figure 16) reveals an upward trend in consecutive dry days, with projections indicating an increase of 13 days per 150 years (about 3 days every 30 years) without rain. This trend aligns with the expected decrease in annual rainfall, which is projected to decline by 253 mm over 150 years or 63 mm every 30 years.

In contrast, daily rainfall intensity has increased, both for single-day and five-day periods. Figure 17 shows that extreme one-day rainfall is expected to rise by 9 mm over 150 years (2 mm per 30 years). Similarly, Figure 18 illustrates that extreme five-day rainfall is projected to increase by 17 mm per 150 years (4 mm per 30 years).

Overall, the five CMIP6 models project that between 2030 and 2099, there will be longer dry periods, fewer rainy days, and reduced annual rainfall. However, when rain does occur, it will be more intense, with increases in both daily and five-day rainfall totals. This suggests that rainfall events will become less frequent but more extreme, resulting in longer dry seasons punctuated by high-intensity rainfall events. When compared to data from 39 rainfall stations, the bias-corrected daily rainfall output from the CMIP6 model for 1980–2014 demonstrates strong performance. Therefore, the CMIP6 model's daily rainfall projections for 2024–2100 can be reliably used as a reference for future rainfall analysis.

4.3. Modeling of Rainfall- Runoff with HEC-HMS

Daily rainfall data from the CMIP6 model for the projection period (2015–2100) were used as the primary reference for assessing future rainfall conditions in runoff modeling with HEC-HMS. Below are the results of the hydrological analysis and the calibration of the model outputs:

4.3.1. Hydrological Analysis and Calibration of Modeling Results with Ground Station Flow Data

The schematic diagram of the Sekampung river basin highlights five key water resource infrastructures in Lampung Province that are the focus of this study: Batutegi Dam, Way Sekampung Dam, Argoguruh Weir, Margatiga Dam, and Jabung Weir. The research area and distribution of rainfall stations are presented in Figure 20.

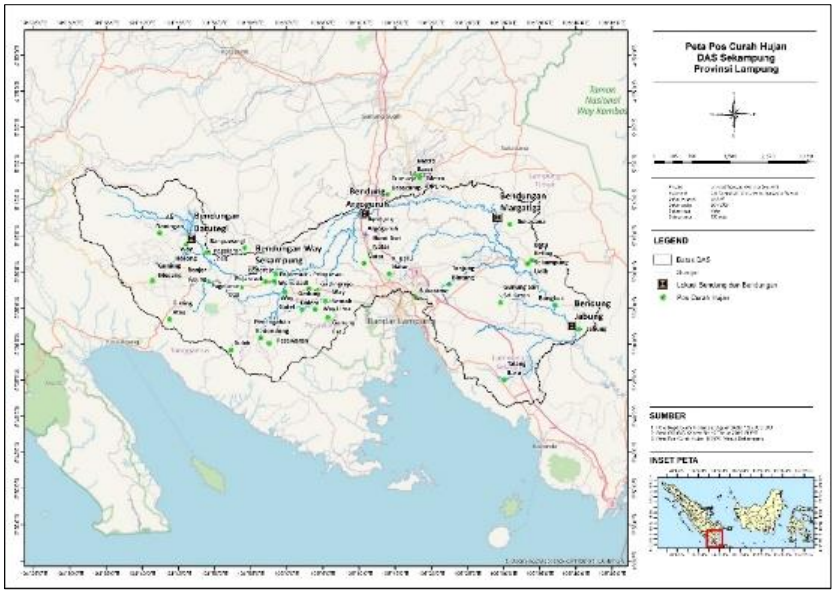

Figure 20. Research Area and Distribution of Rainfall Station

The characteristic data of the Sekampung river basin and the rainfall data collected were then used to build the HEC-HMS model, as shown in Figure 21. The number of sub-watersheds was divided into 62 sub-watersheds, with different parameters for each sub-watershed to suit the land use conditions and soil types in each area.

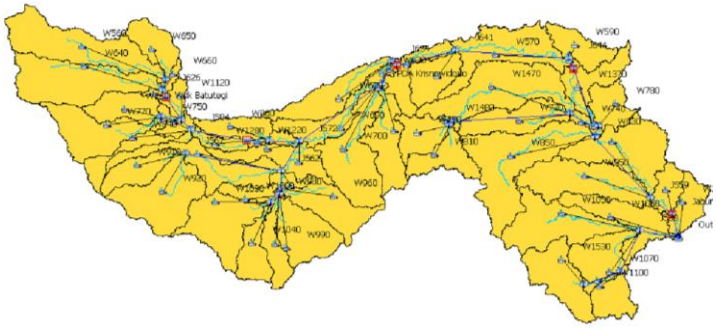

Figure 21. Sub-Watersheds HEC-HMS Model

To obtain satisfactory results, the analysis method used needs to be adjusted according to the desired calculation, in this case, water availability. According to the HEC-HMS usage guidelines, the analysis model for calculating water availability is the Soil Moisture Accounting method for losses, combined with the baseflow method using a linear reservoir [35].

Model calibration was conducted at four water gauge locations (Figures 22 to 25) that were not affected by water regulation by infrastructure and represented the characteristic conditions of the Sekampung river basin from upstream to downstream. These water gauges were located at the Way Kendis-Tegalega, Way Ketibung-Sidomulyo, and Batutegi Dam inflow sites. The following are the calibration graphs and objective parameters for each calibration point:

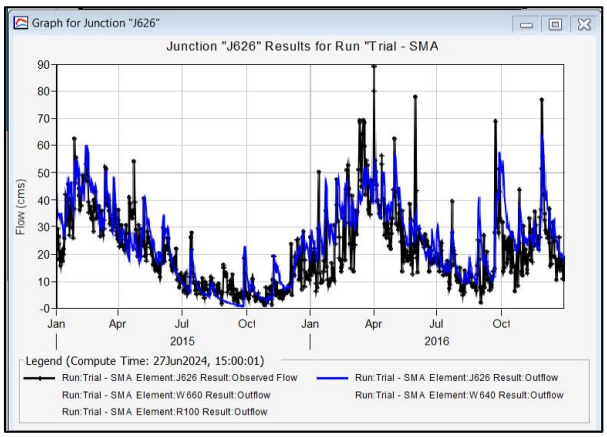

Figure 22. Discharge Calibration at Batutegi Dam site

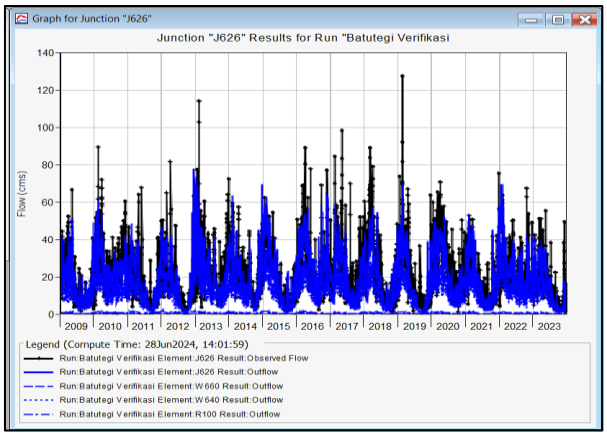

Figure 23. Discharge Verification at Batutegi Dam

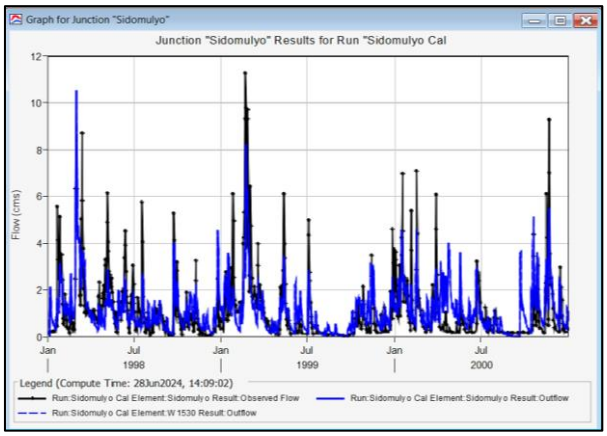

Figure 24. Discharge Calibration at Way Ketibung-Sidomulyo

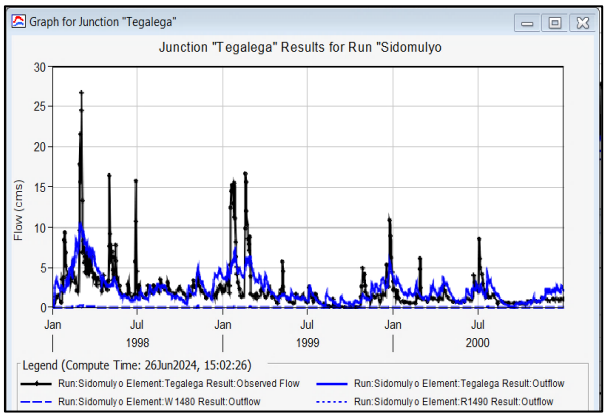

Figure 25. Discharge Calibration at Way Kendis-Tegalega

The calibration results (Table 3) indicate that the objective modeling parameters are reliable and can be used for generating and projecting discharge data. This is evident from the overlapping observation and simulation graphs and statistically demonstrated by the NSE and PBIAS values, as recommended by the ASCE Task Committee in 1993.

Table 3. Results of NSE and PBIAS Values for Calibration

No.	Calibration	NSE	PBIAS
1	Discharge Calibration at Batutegi Dam site	0.609	13.54%
2	Discharge Verification at Batutegi Dam	0.455	8.09%
3	Discharge Calibration at Way Ketibung-Sidomulyo	0.494	7.04%
4	Discharge Calibration at Way Kendis-Tegalega	0.416	7.43%

The NSE values in this calibration range from 0.416 to 0.609, while the PBIAS values range from 7% to 13%. Referring to the size proximity classification according to Moriasi and Cabrera, the calibration results fall within the Good to Very Good criteria. The calibrated model was then used to generate local discharge for each weir and dam using ground rainfall, which was then referred to as the baseline scenario for the period from 1980 to 2023 (Figure 26). The following are the results of local discharge generation for each weir and dam.

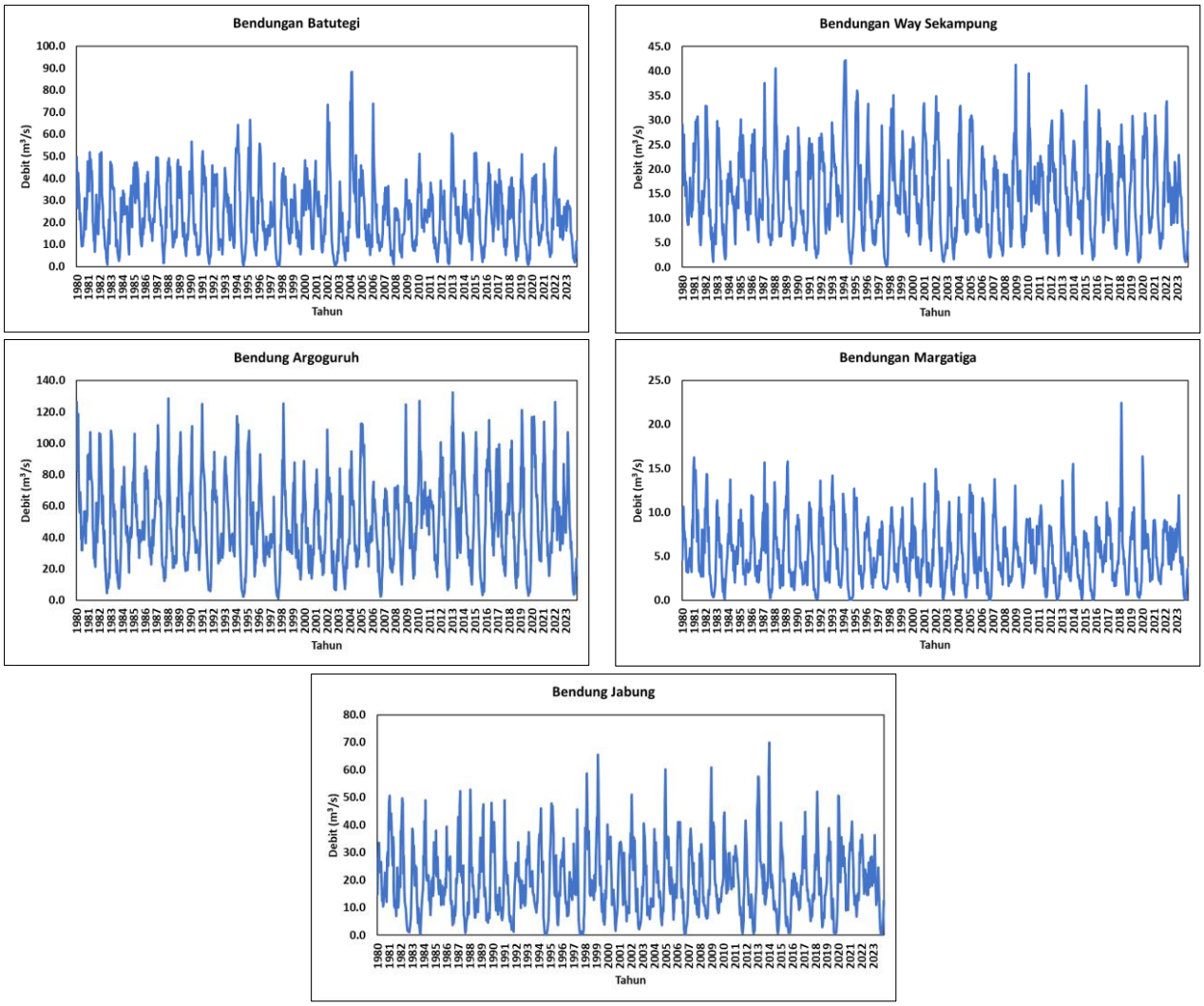

Figure 26. Biweekly Discharge of Dams and Reservoirs in the Sekampung River Basin

The development of operational patterns necessitates adjustments to future climate conditions to optimize water allocation in the river system. Therefore, further simulations are necessary to predict the discharge that will occur in the coming years (2024–2100) using rainfall data generated by CMIP6 climate models, such as MPI-ESM2-LR, MPI-ESM2-HR, Miroc6, CanESM5, and CESM2, for each scenario.

4.3.2. Analysis of Existing Dependable Flow and Projections

The results of calculations for each climate model, namely MPI2LR, MPI2HR, Miroc6, CanESM5, and CESM2, were then summarized into daily dependable flow to determine the extent of change compared to existing models for each water resource infrastructure system in the Sekampung river basin (Batutegi System cascade dam). The following are the changes between the existing dependable flow and the projected dependable flow:

The results of discharge analysis at the Batutegi dam show that, in general, the five climate models indicate a decrease in discharge for low durations (Q1% to Q20%) over the next 100 years. For the MPI2HR, MPI2LR, Microc6, CanESM5, and CESM2 models, the projected discharge from 2024 to 2100 (46.0 to 32.8 m³/second) has decreased compared to the existing discharge from 1980 to 2023 (67.4 to 35.6 m³/second). For medium-duration discharge (Q30% to Q70%), there is an increase in discharge compared to existing discharge for each model. The existing discharge of (30.0 to 12.8) m^3/second increased in all five models by (31.7 to 15.3) m^3/second. Meanwhile, the discharge for high duration (Q80% to Q100%) shows an increase compared to the existing discharge for each model. For the existing discharge of (9.4 to 0.1) m^3/second, there was an increase in all five models of (15.2 to 0.2) m^3/second. Changes in existing discharge and the five models at the Batutegi Dam are illustrated in Figure 27 and summarized in Table 4.

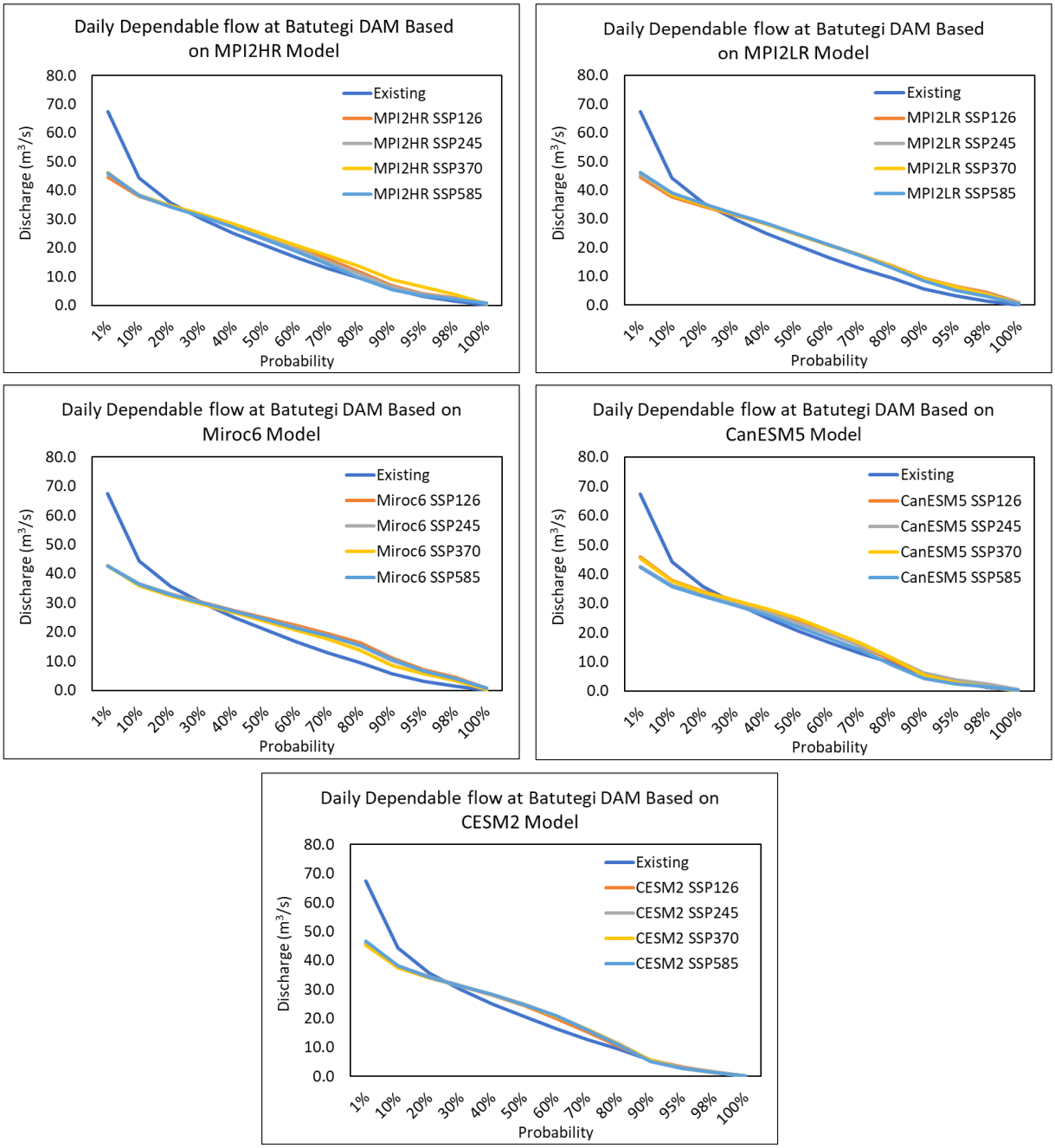

Figure 27. Duration curve of discharge for 5 climate models for the Batutegi Dam

Table 4. Changes in Dependable flow Across Average Scenario Models at Batutegi Dam

Prob (%)	Existing (m^3/s)	MPI2HR (m^3/s)	MPI2LR (m^3/s)	Miroc6 (m^3/s)	CanESM5 (m^3/s)	CESM2 (m^3/s)
1%	67.4	45.6	45.6	42.8	44.0	46.0
10%	44.3	38.2	38.4	36.3	36.8	38.0
20%	35.6	34.6	34.8	32.8	33.3	34.2
30%	30.0	31.3	31.7	30.0	30.4	31.2
40%	25.0	27.8	28.4	27.1	27.4	28.2
50%	20.7	23.9	24.7	24.2	23.6	24.8
60%	16.6	19.8	20.9	21.4	19.5	20.6
70%	12.8	15.7	17.3	18.6	15.3	16.0
80%	9.4	11.4	13.4	15.2	10.4	10.9
90%	5.7	7.0	9.0	10.1	5.4	5.5
95%	3.2	4.5	6.1	6.5	3.1	3.0
98%	1.4	2.7	3.8	4.0	1.7	1.5
100%	0.1	0.7	0.7	0.6	0.3	0.2

The results of the discharge analysis at the Way Sekampung dam show that, in general, the five climate models indicate a decrease in discharge for low durations (Q1% to Q20%) over the next 100 years. For the MPI2HR, MPI2LR, Microc6, CanESM5, and CESM2 models, the projected discharge for 2024-2100 (33.3 to 23.7 m^3/second) has decreased compared to the existing discharge for 1980-2023 (38.2 to 22.8 m^3/second). For medium-duration discharge (Q30% to Q70%), there is an increase in discharge compared to existing discharge for each model. The existing discharge of (19.2 to 9.1) m^3/second increased in all five models to (22.9 to 11.0) m^3/second. Meanwhile, the discharge for high duration (Q80% to Q100%) shows an increase compared to the existing discharge for each model. For the existing discharge of (6.8 to 0.2) m^3/second, there was an increase in all five models of (11.0 to 0.2) m^3/second. Changes in existing discharge and the five models at Way Sekampung Dam are illustrated in Figure 28 and summarized in Table 5.

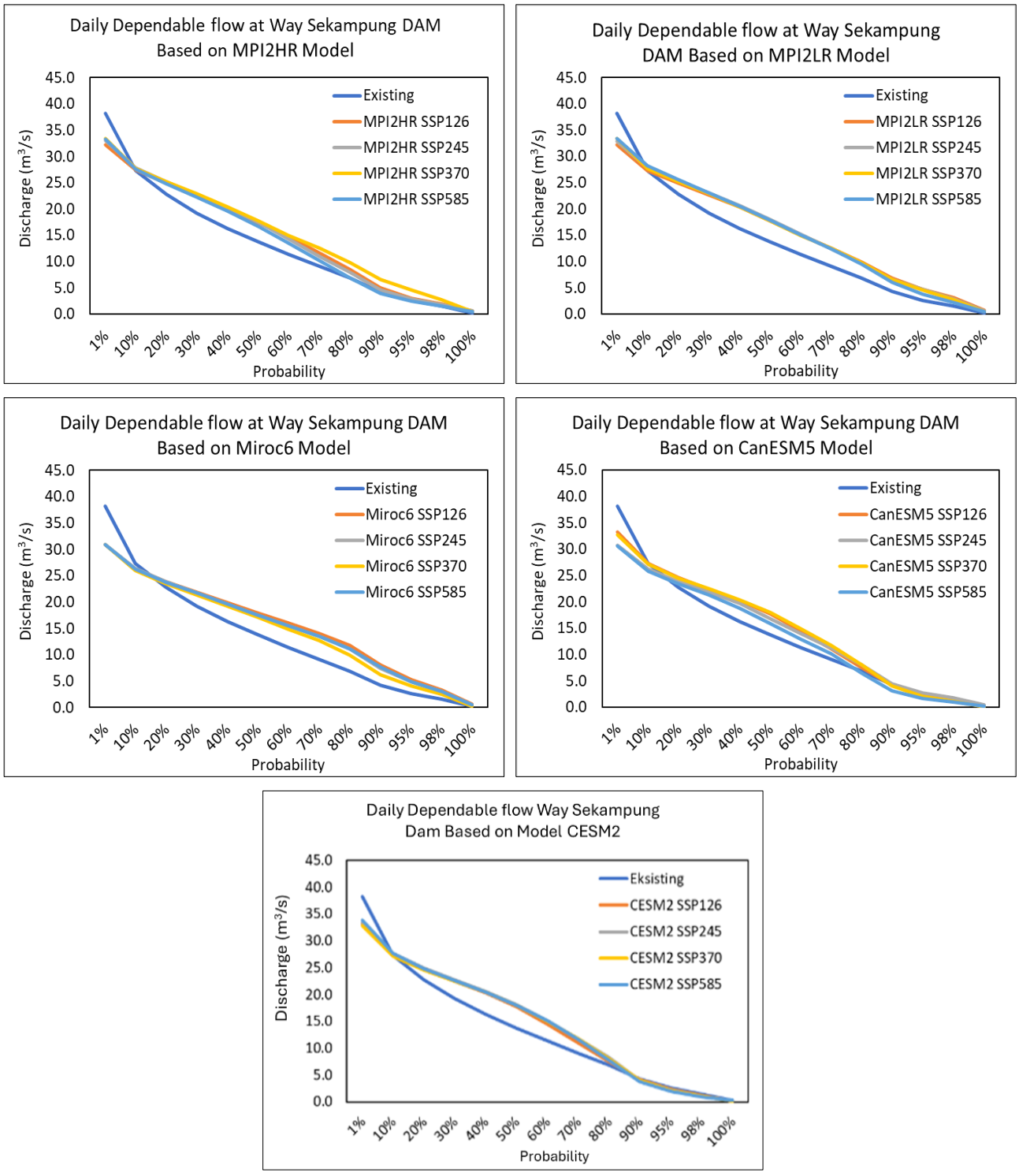

Figure 28. Duration curve of discharge for 5 climate models for the Way Sekampung Dam

Table 5. Changes in Dependable flow Across Average Scenario Models at Way Sekampung Dam

Prob (%)	Existing (m^3/s)	MPI2HR (m^3/s)	MPI2LR (m^3/s)	Miroc6 (m^3/s)	CanESM5 (m^3/s)	CESM2 (m^3/s)
1%	38.2	33.0	33.0	30.9	31.8	33.3
10%	27.3	27.6	27.7	26.2	26.6	27.4
20%	22.8	25.0	25.2	23.7	24.1	24.7
30%	19.2	22.6	22.9	21.7	22.0	22.5
40%	16.3	20.1	20.5	19.6	19.8	20.4
50%	13.7	17.3	17.8	17.5	17.1	17.9
60%	11.3	14.3	15.1	15.4	14.1	14.9
70%	9.1	11.3	12.5	13.4	11.0	11.6
80%	6.8	8.2	9.7	11.0	7.5	7.9
90%	4.3	5.0	6.5	7.3	3.9	4.0
95%	2.6	3.2	4.4	4.7	2.2	2.2
98%	1.5	2.0	2.7	2.9	1.3	1.1
100%	0.2	0.5	0.5	0.4	0.2	0.2

The results of the discharge analysis at the Argoguruh dam indicate that, in general, the five climate models predict an increase in discharge for low durations (Q1% to Q20%) over the next 100 years. For the MPI2HR, MPI2LR, Microc6, CanESM5, and CESM2 models, the projected discharge for 2024-2100 (136.9 to 97.5 m³/second) has increased compared to the existing discharge for 1980-2023 (125.6 to 73.6 m³/second). For medium-duration discharge (Q30% to Q70%), there is an increase in discharge compared to existing discharge for each model. The existing discharge of (62.3 to 31.6) m^3/second increased in the five models by (94.1 to 45.2) m^3/second. Meanwhile, the discharge for high duration (Q80% to Q100%) shows an increase compared to the existing discharge for each model. For the existing discharge of (24.4 to 0.8) m^3/second, there was an increase in the five models of (44.9 to 0.6) m^3/second. Changes in existing discharge and the five models at the Argoguruh Dam are illustrated in Figure 29 and summarized in Table 6.

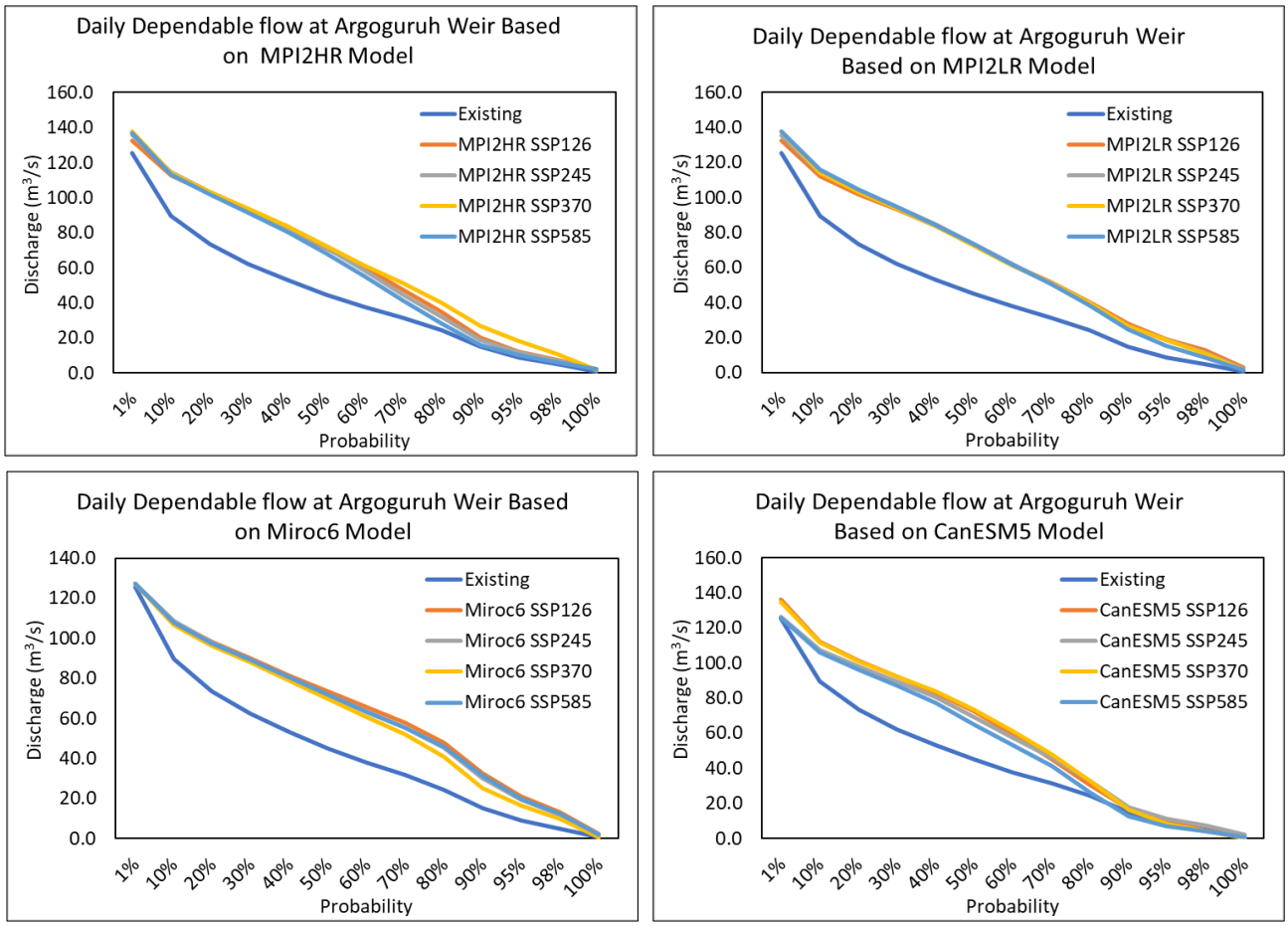

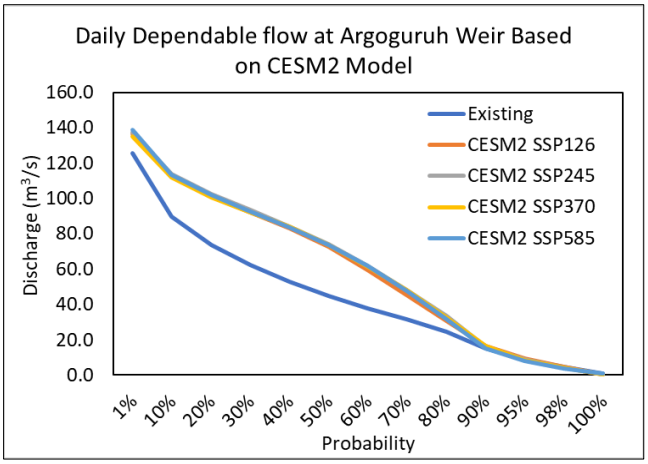

Figure 29. Duration curve of discharge for 5 climate models for the Argoguruh Weir

Table 6. Changes in Dependable flow Across Average Scenario Models at Argoguruh Weir

Prob (%)	Existing (m^3/s)	MPI2HR (m^3/s)	MPI2LR (m^3/s)	Miroc6 (m^3/s)	CanESM5 (m^3/s)	CESM2 (m^3/s)
1%	125.6	135.7	135.7	127.2	130.9	136.9
10%	89.7	113.6	114.1	107.8	109.4	112.8
20%	73.6	102.7	103.6	97.5	99.1	101.6
30%	62.3	92.9	94.1	89.0	90.4	92.6
40%	53.1	82.4	84.2	80.3	81.2	83.7
50%	45.0	70.9	73.1	71.8	70.1	73.5
60%	37.8	58.8	61.8	63.3	57.9	61.2
70%	31.6	46.4	51.1	55.0	45.2	47.4
80%	24.4	33.7	39.5	44.9	30.7	32.2
90%	15.1	20.4	26.6	29.8	15.9	16.1
95%	8.9	13.0	18.0	19.2	9.0	8.7
98%	5.0	8.0	11.0	11.8	5.1	4.3
100%	0.8	2.1	2.1	1.8	0.9	0.6

The results of the discharge analysis at the Margatiga dam indicate that, in general, the five climate models predict an increase in discharge for low durations (Q1% to Q20%) over the next 100 years. For the MPI2HR, MPI2LR, Microc6, CanESM5, and CESM2 models, the projected discharge for 2024-2100 (15.5 to 10.8 m³/second) has increased compared to the existing discharge for 1980-2023 (15.3 to 8.3 m³/second). For medium-duration discharge (Q30% to Q70%), there is an increase in discharge compared to existing discharge for each model. The existing discharge of (7.0 to 3.0) m^3/second increased in all five models to (10.4 to 4.7) m^3/second. Meanwhile, the discharge for high duration (Q80% to Q100%) shows an increase compared to the existing discharge for each model. For the existing discharge of (2.2 to 0.0) m^3/second, there was an increase in all five models of (4.6 to 0.0) m^3/second. Changes in existing discharge and the five models at the Margatiga Dam are illustrated in Figure 30 and summarized in Table 7.

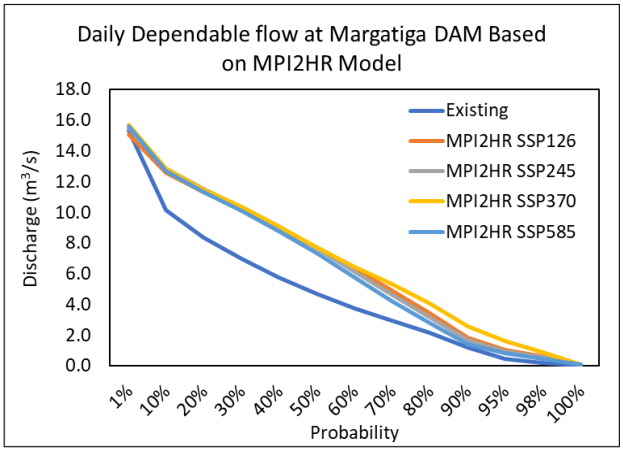

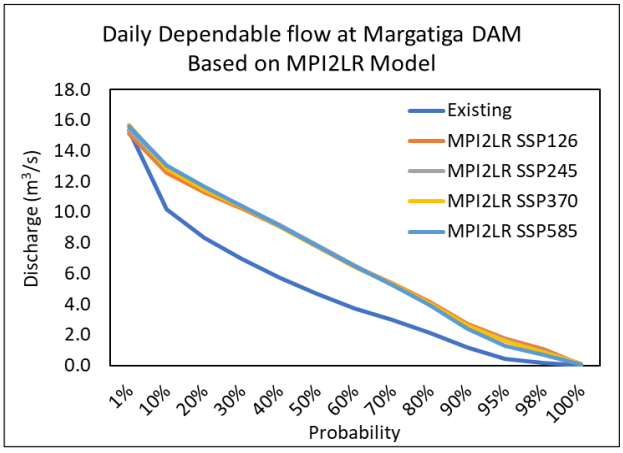

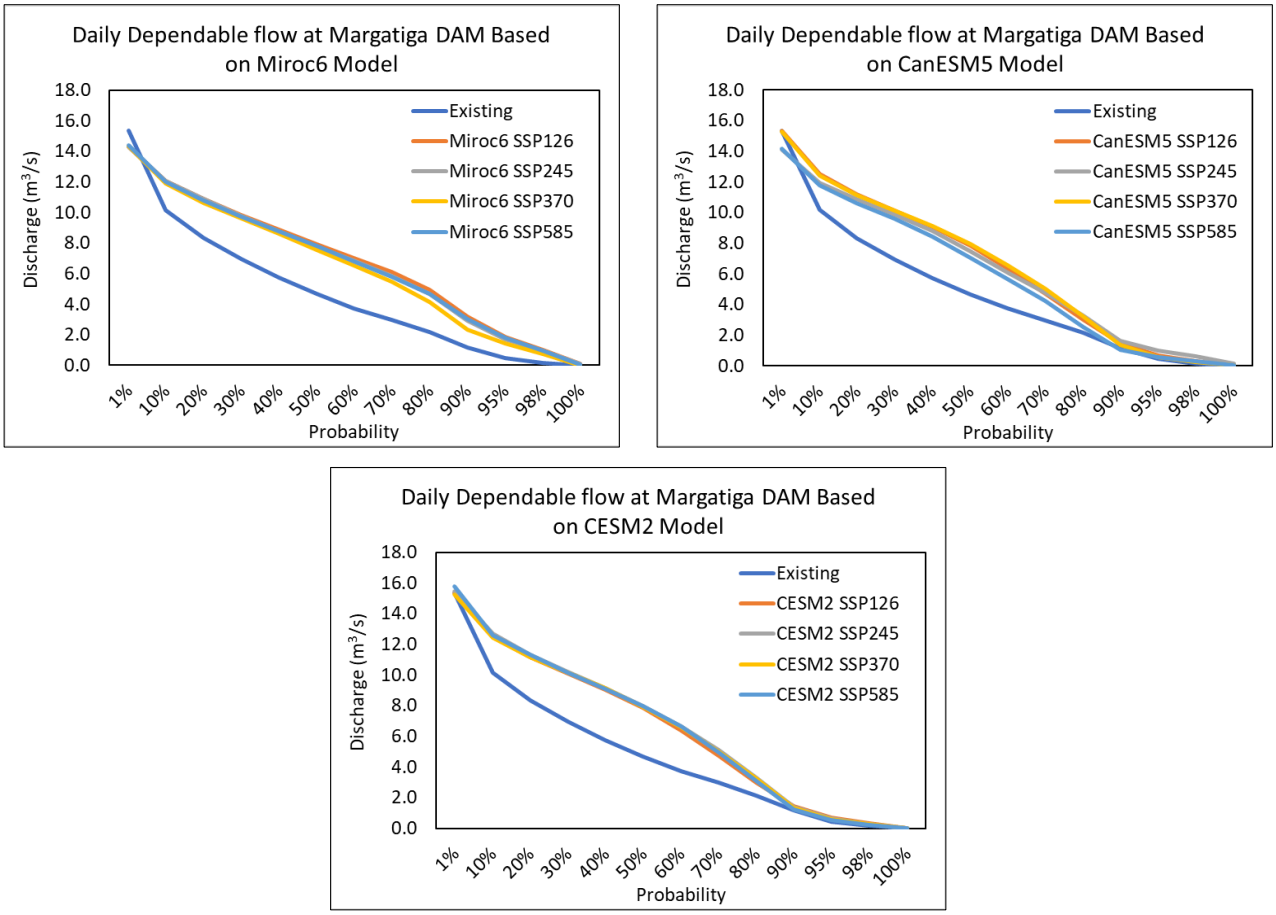

Figure 30. Duration curve of discharge for 5 climate models for the Margatiga Dam

Table 7. Changes in Dependable flow Across Average Scenario Models at Margatiga Dam

Prob (%)	Existing (m^3/s)	MPI2HR (m^3/s)	MPI2LR (m^3/s)	Miroc6 (m^3/s)	CanESM5 (m^3/s)	CESM2 (m^3/s)
1%	15.3	15.5	15.5	14.3	14.7	15.5
10%	10.2	12.7	12.8	12.0	12.2	12.6
20%	8.3	11.4	11.5	10.8	10.9	11.2
30%	7.0	10.2	10.4	9.7	9.9	10.2
40%	5.7	8.9	9.1	8.7	8.9	9.1
50%	4.7	7.6	7.8	7.8	7.6	7.9
60%	3.7	6.2	6.5	6.8	6.2	6.6
70%	3.0	4.8	5.3	5.8	4.7	4.9
80%	2.2	3.3	4.0	4.6	3.0	3.2
90%	1.2	1.9	2.6	2.9	1.4	1.4
95%	0.5	1.1	1.6	1.7	0.7	0.6
98%	0.2	0.6	0.9	0.9	0.4	0.3
100%	0.0	0.1	0.1	0.1	0.1	0.0

The results of the discharge analysis at the Jabung movable dam indicate that, in general, the five climate models predict a decrease in discharge for low durations (Q1% to Q20%) over the next 100 years. For the MPI2HR, MPI2LR, Microc6, CanESM5, and CESM2 models, the projected discharge for 2024-2100 (51.0 to 35.6 m³/second) has decreased compared to the existing discharge for 1980-2023 (55.3 to 29.5 m³/second). For medium-duration discharge (Q30% to Q70%), there is an increase in discharge compared to existing discharge for each model. The existing discharge of (24.5 to 11.5) m^3/second increased in all five models by (34.1 to 15.4) m^3/second. Meanwhile, the discharge for high duration (Q80% to Q100%) shows an increase compared to the existing discharge for each model. For the existing discharge of (8.3 to 0.0) m^3/second, there is an increase in all five models of (15.2 to 0.1) m^3/second. Changes in existing discharge and the five models at the Jabung Movable Weir are illustrated in Figure 31 and summarized in Table 8.

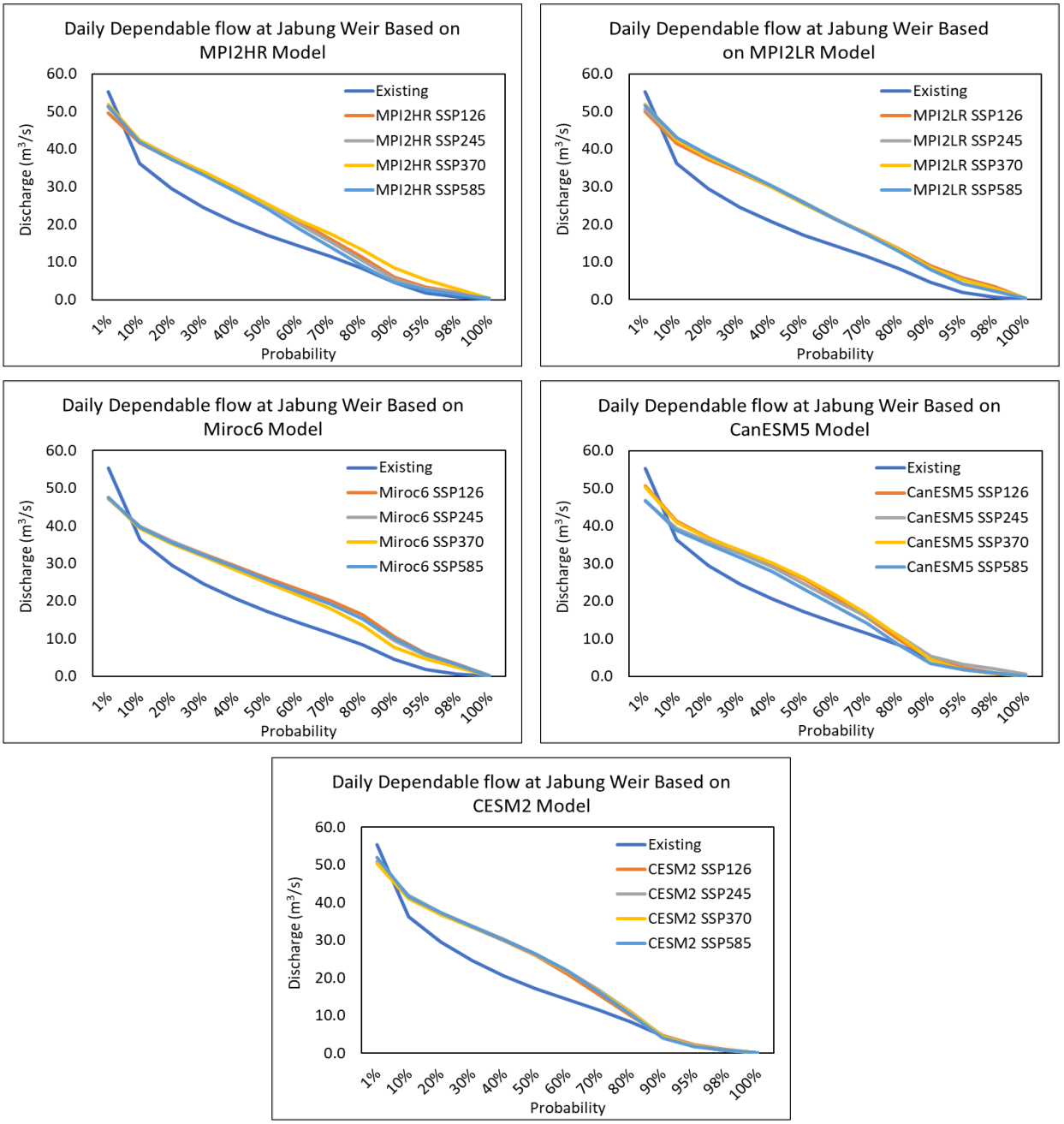

Figure 31. Duration curve of discharge for 5 climate models for the Jabung Weir

Table 8. Changes in Dependable Discharge across Average Scenario Models at Jabung Weir

Prob (%)	Existing (m^3/s)	MPI2HR (m^3/s)	MPI2LR (m^3/s)	Miroc6 (m^3/s)	CanESM5 (m^3/s)	CESM2 (m^3/s)
1%	55.3	51.0	51.0	47.3	48.6	51.0
10%	36.3	42.0	42.3	39.6	40.1	41.4
20%	29.5	37.6	37.9	35.6	36.1	37.1
30%	24.5	33.7	34.1	32.1	32.7	33.5
40%	20.6	29.5	30.0	28.8	29.2	30.0
50%	17.2	25.1	25.7	25.6	25.0	26.2
60%	14.3	20.3	21.4	22.4	20.4	21.6
70%	11.5	15.7	17.4	19.1	15.4	16.3
80%	8.3	11.0	13.2	15.2	9.9	10.4
90%	4.6	6.2	8.5	9.4	4.5	4.5
95%	1.8	3.6	5.2	5.6	2.3	2.0
98%	0.7	2.0	3.0	2.9	1.2	0.8
100%	0.0	0.3	0.3	0.2	0.2	0.1

Synthetic discharge, which has been carried out in the Sekampung river basin using runoff rainfall modeling, has been calibrated against observed discharge. The modeling was used to determine the extent of changes in flow discharge resulting from climate change, incorporating rainfall scenarios from various climate models and projections for the period up to 2100. The results of daily discharge data predictions indicate that several models show a significant increase, particularly in local discharge during high discharge durations at the Argoguruh Dam, Margatiga Dam, and Jabung Dam. This analysis does not assess which climate model is the best, but rather whether the discharge data used can be adjusted to match the model conditions and climate scenarios suitable for the study location. The results of this study can inform further research to develop recommendations for optimal dam operation patterns.

4.4. Optimization of Reservoir Operation Patterns Due to Climate Change

4.4.1. Technical Data and Planting Patterns

The Batutegi Cascade Dam System in the Sekampung River Basin consists of five important infrastructures, namely: Batutegi Dam (2004), with a storage volume of 690 million m^3; Way Sekampung Dam (2021), with a storage volume of 68 million m^3; Argoguroh Dam (1935) serving the Sekampung irrigation system area with an area of 72,702 ha, Margatiga Dam (2024) with a storage volume of 29.96 million m3, and Jabung Dam (2020) serving the Jabung irrigation area covering 16,588 ha. Generally, the planting season in the above system occurs three times a year, with a planting pattern of rice, followed by rice, and then secondary crops. The following are the existing infrastructure conditions and operating patterns up to the base year 2023: (Figures 32 and 33) [36, 37].

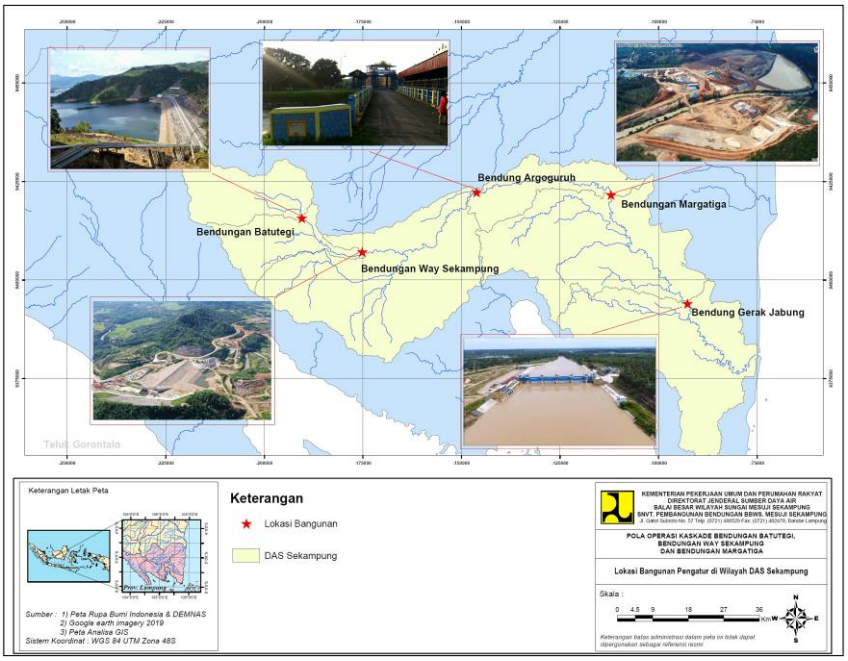

Figure 32. Map of the Sekampung river basin and the locations of control structures on the Way Sekampung River

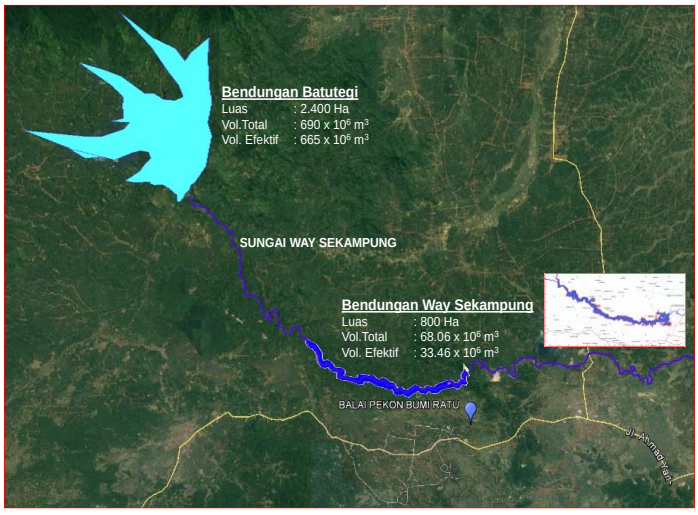

Figure 33. Map showing the shape of the Batutegi Dam, Sekampung Dam, and Margatiga Dam

The base year for the analysis is 2023, which serves as a reference for existing infrastructure conditions and operating patterns up to that year. The hydrological data (rainfall, discharge, and climatology) used in the analysis were selected for the period from 1980 to 2023, based on data availability. The climate change projection year that impacts hydrological data was selected for the period 2024–2100. Infrastructure conditions and operational patterns also change dynamically in response to the dynamics of population growth, environmental changes, political developments, economic fluctuations, societal shifts, cultural transformations, defense, and security concerns. The water allocation scheme for the Sekampung irrigation system and the River Basin scheme of the RIBASIM model is shown in Figures 34 and 35.

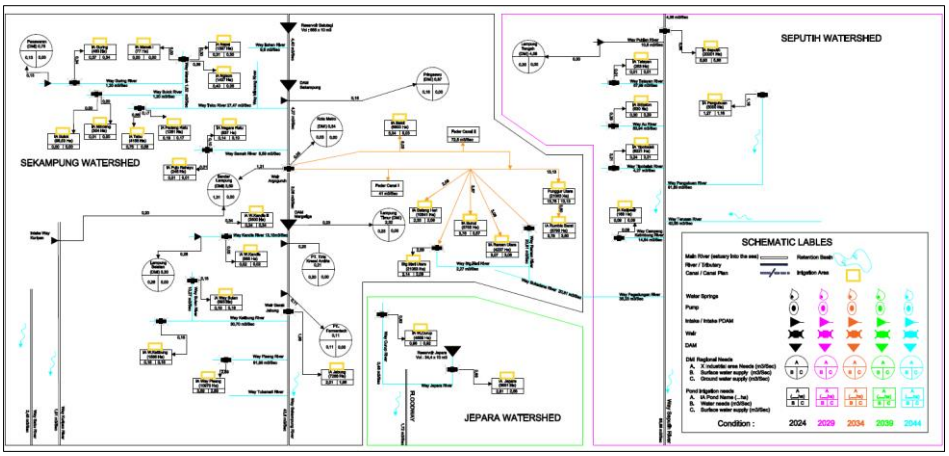

Figure 34. Water allocation scheme for Sekampung system according to pattern [37]

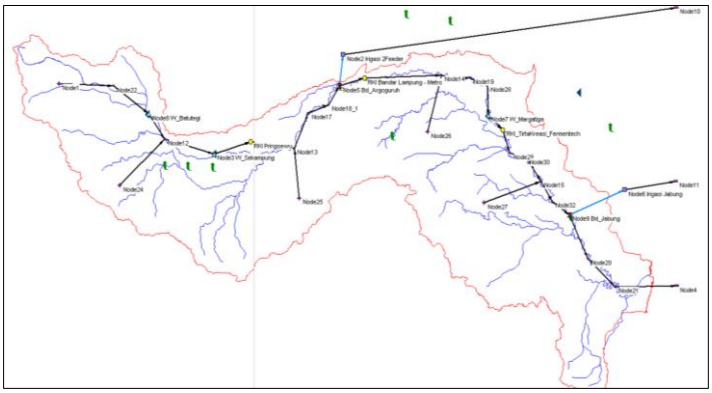

Figure 35. The River Basin scheme of RIBASIM model

Batutegi Reservoir Operation (H-V-A Curve, Electricity, Downstream Demand): When using wet year inflow probability, the TMA will follow the blue line; when using dry year inflow probability, the TMA will follow the red line. Optimization of Way Sekampung Reservoir Operation (H-V-A Curve, Electricity, Downstream Demand) is performed using wet year inflow probability, where the TMA follows the blue-gray line. Conversely, when using the dry year inflow probability, the TMA follows the green line. The following are the curves showing the relationship between storage elevation and inundation area at the Batutegi Cascade System dam (see Figures 36 to 38).

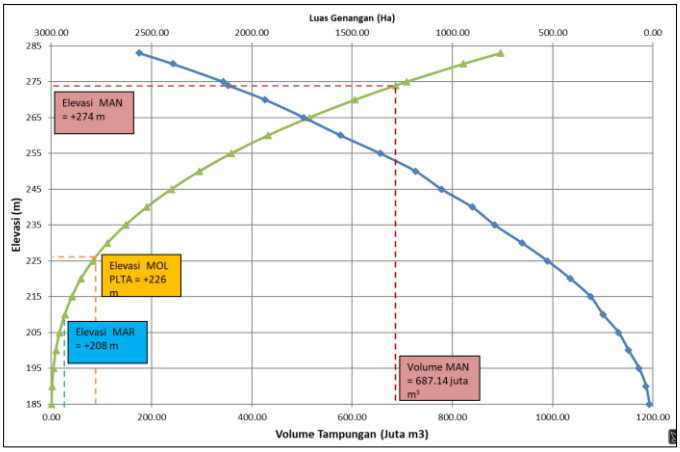

Figure 36. H-V-A curve of Batutegi Reservoir (existing)

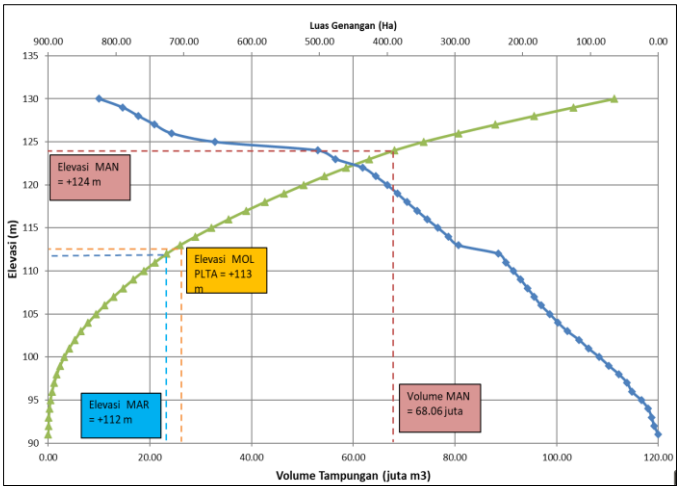

Figure 37. H-V-A curve of the Sekampung Reservoir

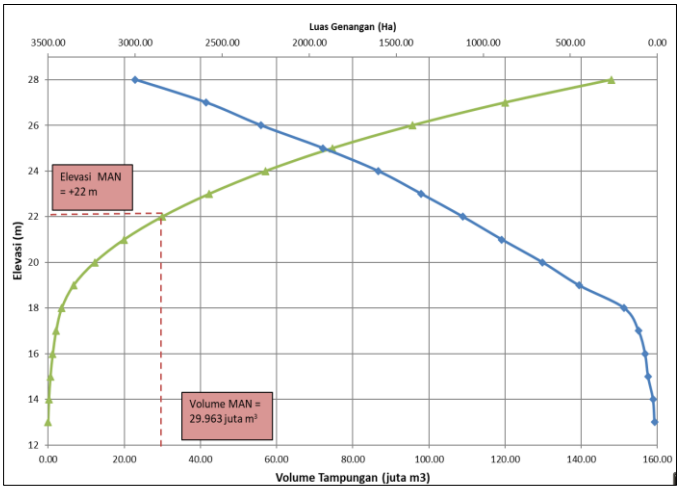

Figure 38. H-V-A curve of Margatiga Reservoir

The Sekampung System Irrigation Area (72,707 ha) comprises several irrigation subsystems covering an area of approximately 55,373 ha, with plans to develop the Rumbia Irrigation Area (17,334 ha). The Sekampung System Irrigation Area (DI) consists of:

- North Punggur System = 21,181 ha
- Rumbia Barat System = 5,106 Ha
- Raman Utara System = 4,216 Ha
- Sekampung Bunut System = 4,871 Ha
- Bekri System = 5,000 Ha
- Batang Hari Utara System = 4,721 Ha
- Sekampung Batang Hari System = 10,278 Ha

Irrigation water is regulated by the Argoguruh Dam through two intakes, namely Feeder Canal I and Feeder Canal II. With the regulation from the Way Sekampung Dam, it is planned to increase planting intensity by 270%. The planting pattern in the Sekampung System Irrigation Area is shown in Figure 39.

In addition to supplying water to the Sekampung Irrigation Area, the system will also irrigate the 5,638-hectare Jabung Kiri Irrigation Area and the potential development of the 10,950-hectare Jabung Kanan Irrigation Area, which is served by the Jabung Movable Dam, with a cropping pattern as shown in Figure 40.

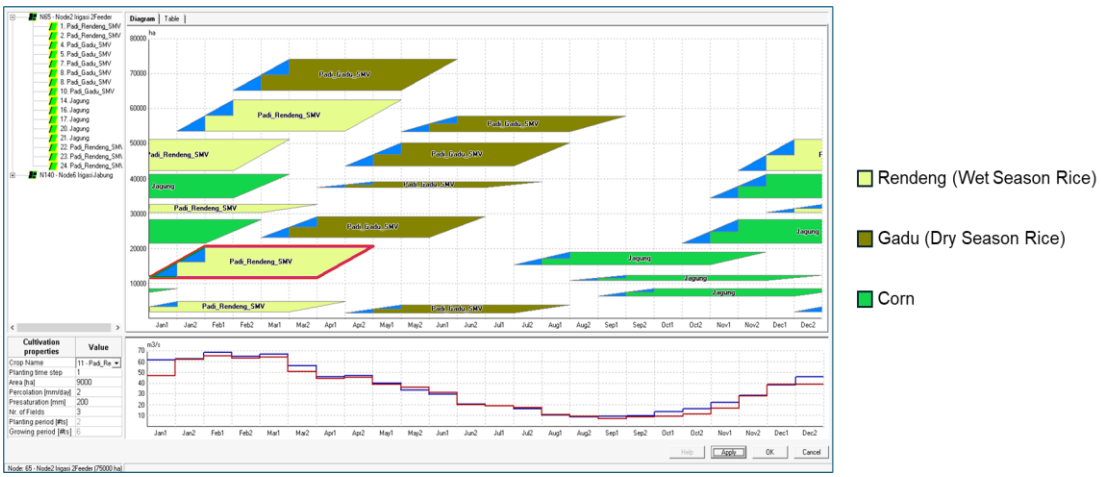

Figure 39. Crop Patterns in the Way Sekampung Irrigation Area. ***Source: Independent Optimization Analysis***

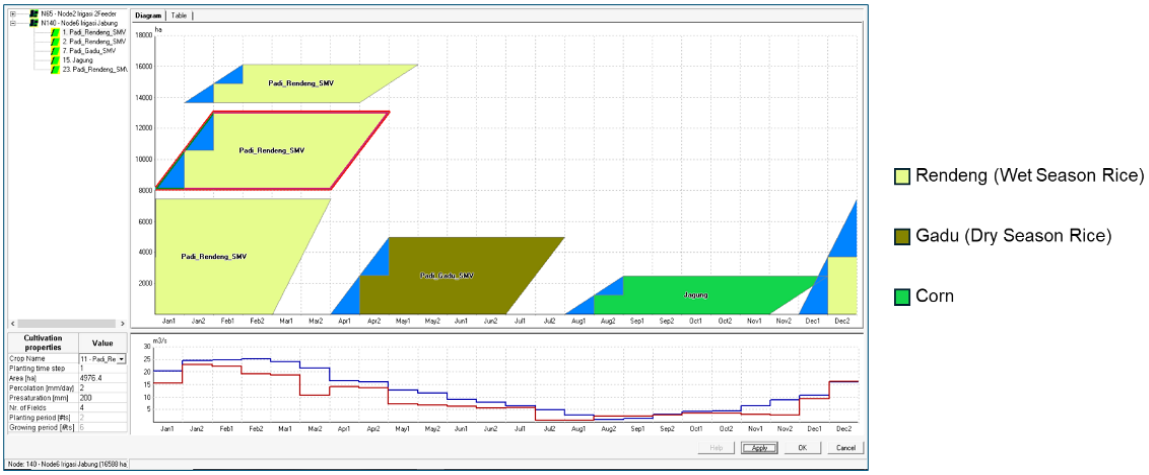

Figure 40. Crop patterns in the Jabung Irrigation Area

4.4.2. Existing Reservoir Operation Patterns

Efficient water release management and adjustments to reservoir operation patterns can maximize storage capacity and maintain sustainable water availability [38]. From an environmental perspective, designing reservoir operation patterns that integrate socio-economic objectives with methane emission mitigation and water quality improvement expands the sustainability dimension of water resource management [39]. From a global perspective, evaluating storage-based operation schemes in 289 reservoirs worldwide found that volume-based models can serve as a generic reference for formulating reservoir operation patterns in various hydrological conditions [40].

The Batutegi Cascade Reservoir system consists of three reservoirs, namely the Batutegi Reservoir with an effective storage capacity of 665 million m^3 (at an elevation between +208 m above sea level and +274 m above sea level) and an effective storage capacity for electricity of 600 million m^3 (at elevations between +226 m and +274 m). Way Sekampung Reservoir has an effective storage capacity of 23.27 million m^3 (at an elevation between +112 m and +124 m) and an effective storage capacity for electricity of 22 million m^3 (at an elevation between +113 m and +124 m). Margatiga Reservoir has an effective storage capacity of 26.77 million m^3 (at an elevation between +17 m dpl and +22 m dpl) and does not have a power plant facility.

Based on the data obtained, the operating patterns of the three reservoirs were not found, so modeling was carried out by constructing reservoir operating patterns based on existing actual Water Level (WL) data and engineering, namely by limiting the most likely normal and extreme reservoir operating patterns by considering several things, namely: actual WL, existing actual fulfilment conditions (irrigation & DMI), electricity production conditions, and the potential area of irrigable land that can be productive. The Resevoir operation simulation evaluation was conducted considering that these reservoirs operate in cascade with the Argoguruh Weir, Jabung Weir, and the DMI water intake infrastructure.

4.4.3. Evaluation Stage of Existing Actual Simulation of High-Water Level

Under these conditions, the Batutegi Reservoir operation pattern follows the high-water level operation pattern based on the actual water level for 2014, as shown in Figure 41.

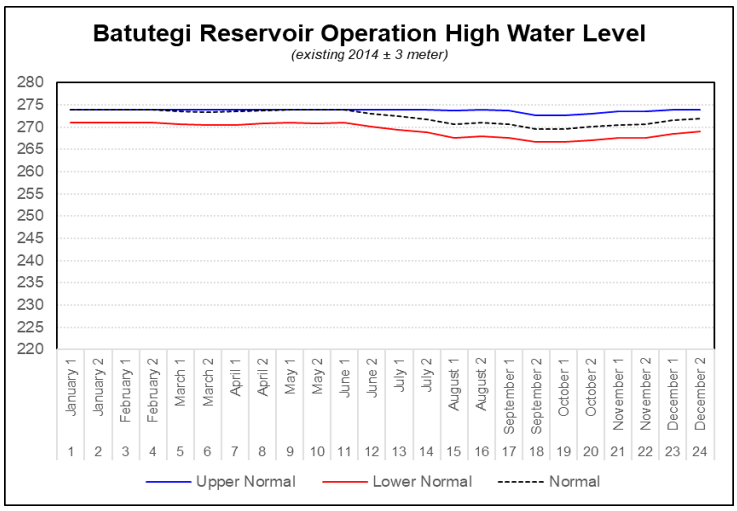

Figure 41. Batutegi Reservoir Operation High Water Level

The Way Sekampung Reservoir follows a high-water-level operation pattern based on the actual water level in 2022, as shown in Figure 42.

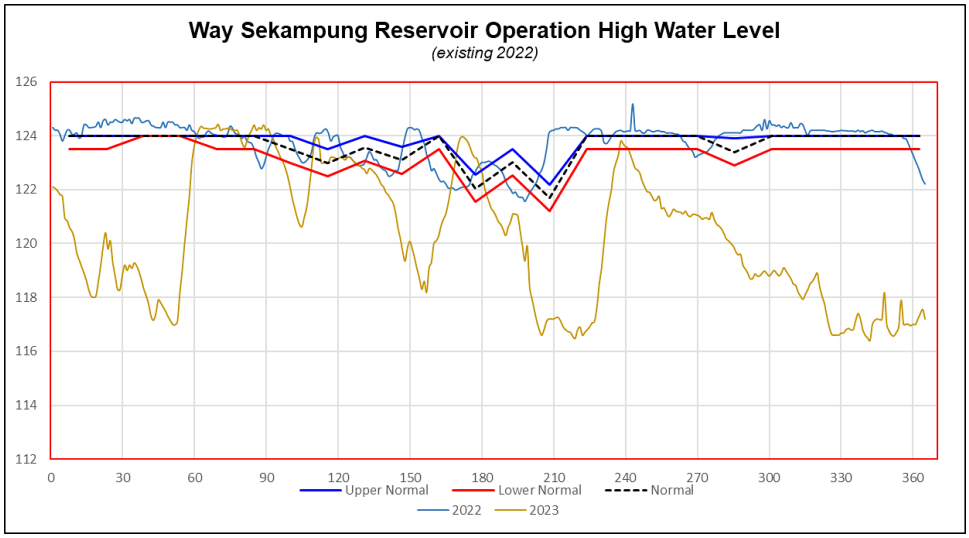

Figure 42. Way Sekampung Reservoir Operation High Water Level

The Margatiga Reservoir does not yet have Reservoir Operation data; therefore, the evaluation of its high-water level operations is based on the maximum water level at the spillway elevation. The normal operating target is set at 2 meters below the spillway elevation, and the lower normal operating level is defined as 2 meters below the normal target, as shown in Figure 43.

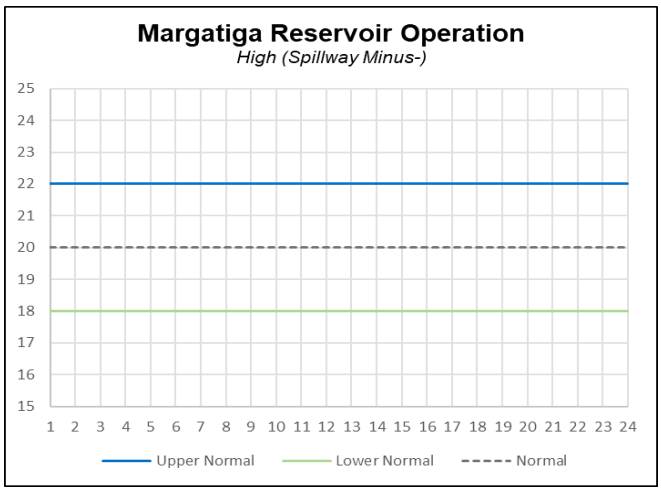

Figure 43. Margatiga Reservoir Operation

The response of the Sekampung water management system with the high water level reservoir operation as described above provides several values as presented in Table 9.

Table 9. Evaluation response to high water levels in high reservoir operation

Infrastructure	Success (%)	Energy (GWH)	Utilization (%)	Shortage Demand (m^3/det)
Batutegi Dam	96,5	193.8	77.4	
Sekampung Dam	100	2.7	100	
Way Sekampung Irrigation Area	99.8		37.1	
Margatiga Dam			0.5	
Jabung Irrigation Area	100		10.4	
Pringsewu DMI	100			0
Lampung Metro DMI	99.8			0
TtrKreasi_Fermnt DMI	100			0

4.4.4. Existing Simulation Evaluation Stage Low Water Level

Under these conditions, the Batutegi Reservoir operates according to the low TMA pattern based on the actual TMA for 2012, as shown in Figure 44.

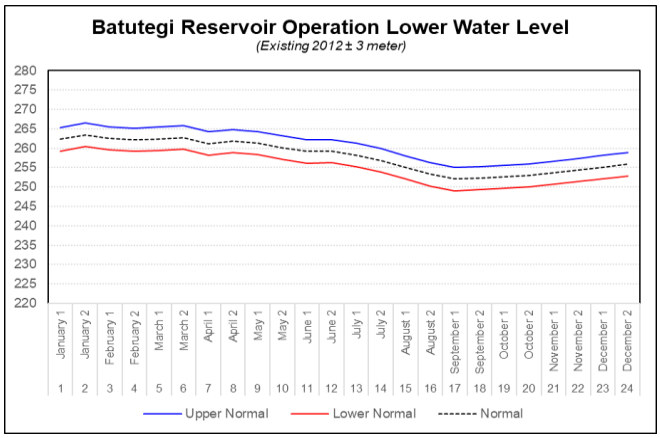

Figure 44. Batutegi Reservoir Operation Low Water Level

The Sekampung Reservoir follows a low water level operation pattern based on the actual water level in 2023 as shown in Figure 45.

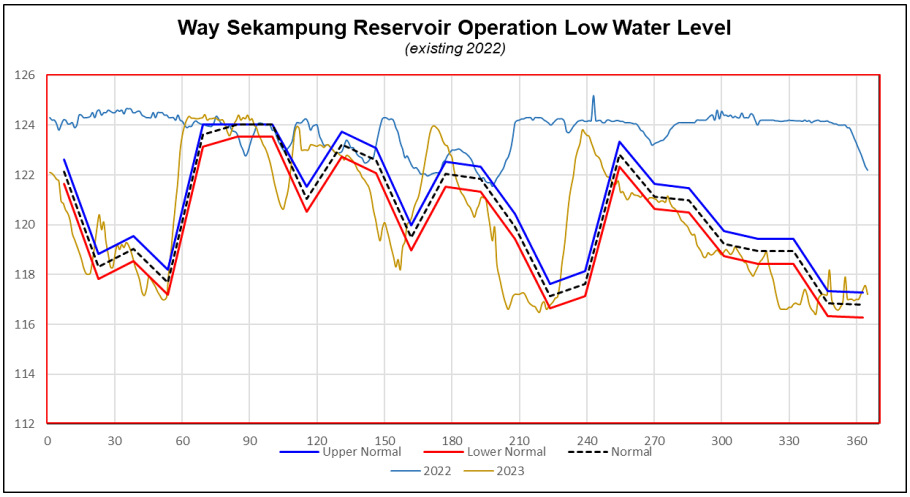

Figure 45. Way Sekampung Reservoir Operation Low Water Level

The Margatiga Reservoir does not yet have standard reservoir operation data, so the actual evaluation of low water level operations is determined based on the lowest water level of operation, which is the lower normal level at the dead storage elevation, and then the normal target is based on 2 meters above the dead storage elevation, and then the upper normal level is 2 meters above the normal target, as shown in Figure 46.

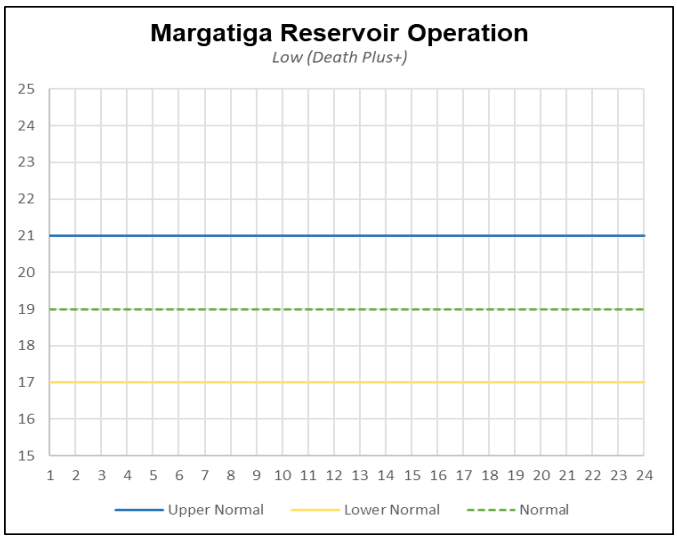

Figure 46. Margatiga Reservoir Operation

The response of the Sekampung water management system with the above low water level reservoir operation pattern provides several values as presented in Table 10.

Table 10. Evaluation response to high water levels in low reservoir operation

Infrastructure	Success (%)	Energy (GWH)	Utilization (%)	Shortage Demand (m^3/det)
Batutegi Dam	91.6	187.9	79.6	
Sekampung Dam	99.5	2.6	100	
Way Sekampung Irrigation Area	99.8		37.0	
Margatiga Dam			0.5	
Jabung Irrigation Area	100		10.3	
Pringsewu DMI	100			0
Lampung Metro DMI	99.2			0
TtrKreasi_Fermnt DMI	100			0

4.4.5. Existing Free Water Level Simulation Evaluation Step

Under these conditions, the Batutegi Reservoir operates according to the free water level pattern, where reservoir operation is constrained within the effective storage elevation limits. The upper normal water level corresponds to the spillway crest elevation, while the lower normal water level is defined by the dead storage elevation. The normal target water level is set at the midpoint elevation between the spillway crest and the dead storage, as illustrated in Figure 47.

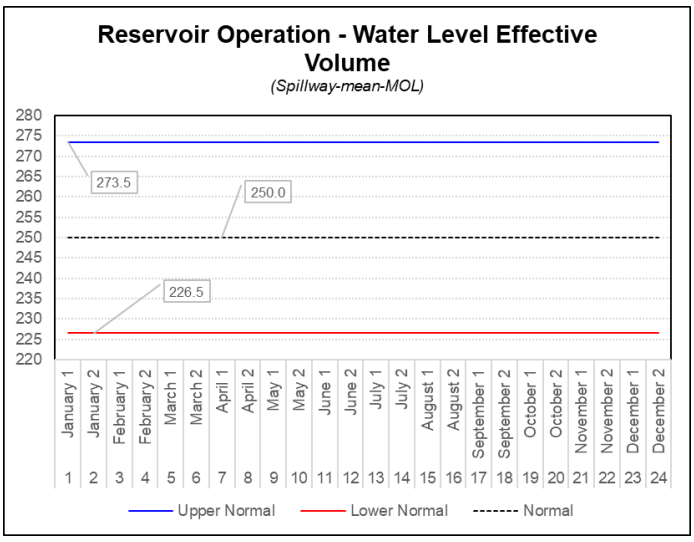

Figure 47. Reservoir Operation – Water Level Effective Volume

The Sekampung Reservoir operates under free water level control, where reservoir operations are maintained within the effective storage elevation limits. The upper normal water level is set at the spillway elevation, the lower normal water level corresponds to the dead storage elevation, and the normal target is defined as the average elevation between the spillway crest and the dead storage, as illustrated in Figure 48.

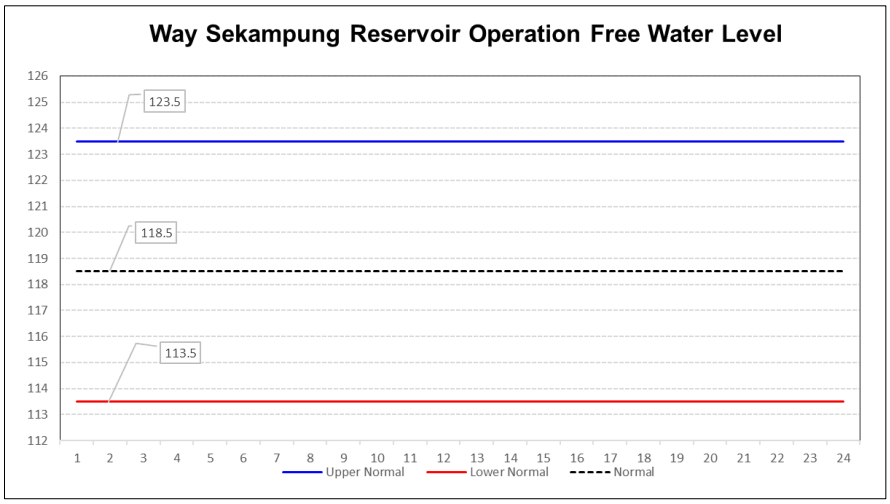

Figure 48. Sekampung Reservoir Operation at Free Water Level

The Margatiga Reservoir does not yet have standardized reservoir operation data; therefore, the actual free water level operation is evaluated based on reservoir operation within the effective storage elevation limits. The upper normal water level is set at the spillway elevation, the lower normal water level corresponds to the dam's dead storage elevation, and the normal target is defined as the average elevation between the spillway crest and the dead storage, as illustrated in Figure 49.

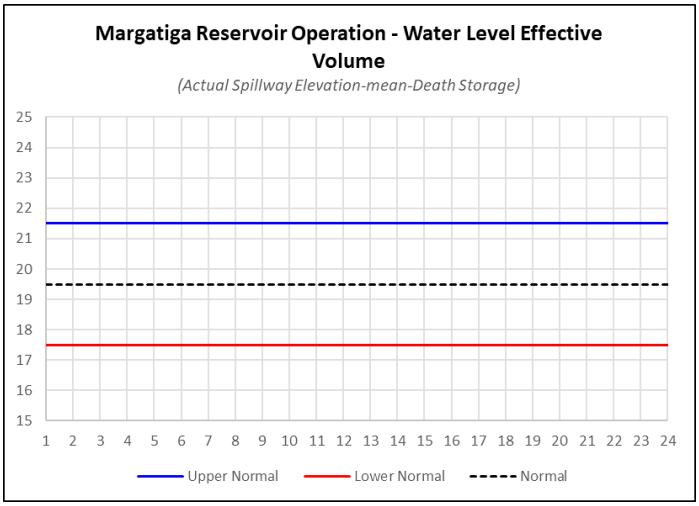

Figure 49. Margatiga Reservoir Operation at Water Level Elevation Effective Volume

The response of the Sekampung water management system with the above low water level reservoir operation pattern provides several values as presented in Table 11.

Table 11. Evaluation response of water level in free dam operation pattern at effective volume elevation

Infrastructure	Success (%)	Energy (GWH)	Utilization (%)	Shortage Demand (m^3/det)
Batutegi Dam	100	228.5	91.6	
Sekampung Dam	100	2.6	100	
Way Sekampung Irrigation Area	100		37.0	
Margatiga Dam			0.5	
Jabung Irrigation Area	100		10.3	
Pringsewu DMI	100			0.0
Lampung Metro DMI	100			0.1
TtrKreasi_Fermnt DMI	100			0.1

4.4.6. Reservoir Simulation Projection

Getahun et al. [41] emphasizes the importance of integrated hydrological modeling that combines target-storage parameters with flow simulations to produce more accurate projections. On the other hand, Lee et al. [42] developed an adaptive framework to improve the resilience of reservoir operation systems to increasingly frequent droughts. Simulation projections were conducted on the Batutegi System cascade reservoirs, specifically the Batutegi Reservoir, Way Sekampung Reservoir, and Margatiga Reservoir, which operate in tandem to maximize the utilization of water from the Sekampung River. There are the Argoguruh Dam, with a total irrigation area and development of 72,707 Hectares, and the Jabung Dam, with a total irrigation area and development of 16,588 Hectares.

4.4.7. Optimization of Reservoir Operation Projections

Optimization of Margatiga Reservoir Operations (H-V-A Curve and Downstream Requirements): When applying the inflow probability for wet years, the reservoir water level follows the blue line, whereas for dry years, it follows the orange line. In defining the Reservoir Operation Pattern, the optimal operation corridor must remain within the Upper and Lower Operation Limits, considering actual inflow and reservoir water levels. The following section presents the optimization results for each reservoir (see Figures 50 to 52):

- **Batutegi Reservoir Operation**

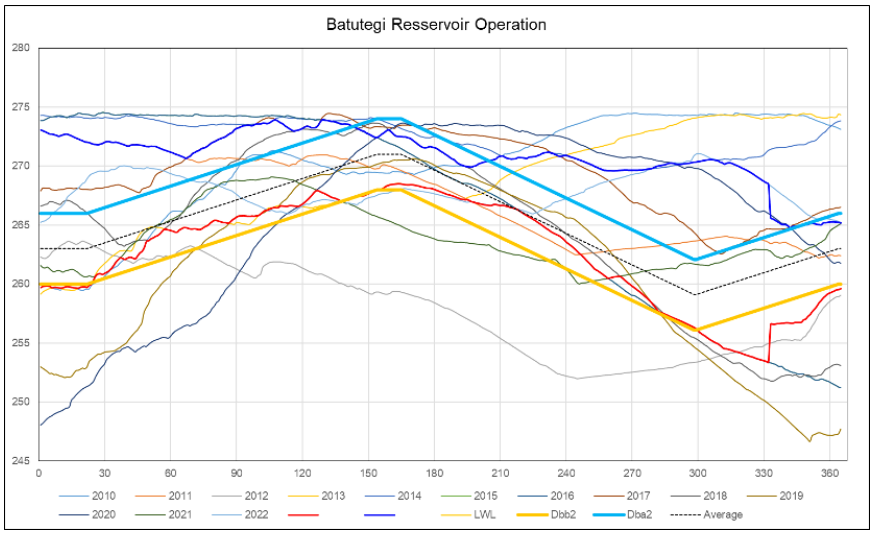

Figure 50. The Batutegi reservoir operation pattern as an upper and lower limit operation corridor

- **Way Sekampung Reservoir Operation**

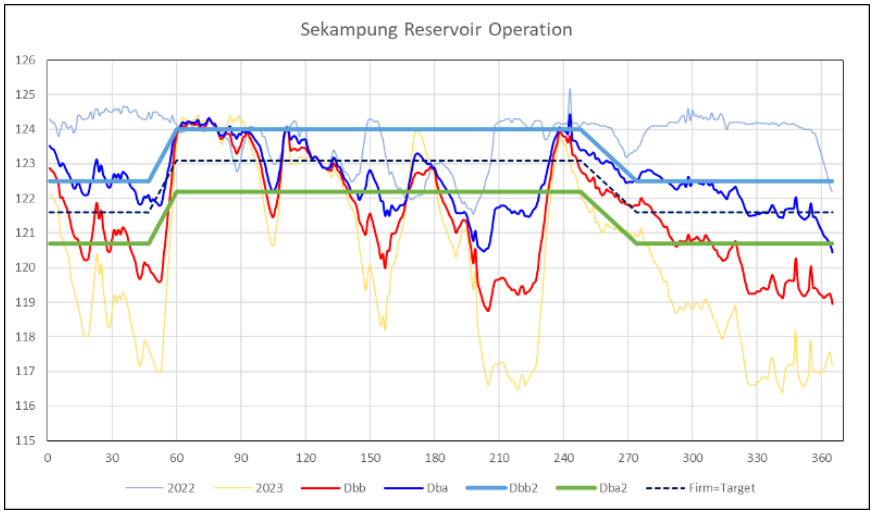

Figure 51. The operation pattern of the Sekampung reservoir as an upper and lower limit operation corridor

- **Margatiga Reservoir Operation**

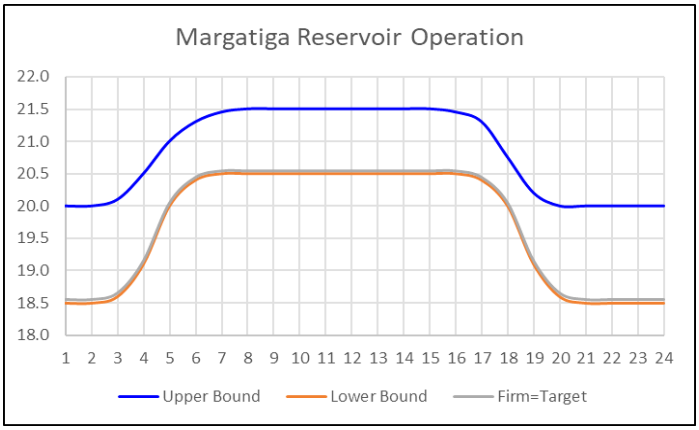

Figure 52. The operation pattern of the Margatiga reservoir as an upper and lower limit operation corridor

4.4.8. Optimization of Water Allocation Balance Model Calibration (Period 1980-2023)

Based on RIBASIM monitoring results, it is shown that the fulfilment (irrigation supply conditions) of water allocation for the Sekampung System and Jabung Irrigation is above 99%, meeting the RKI requirements. Pringsewu, RKI. Lampung-Metro, RKI. Tirtakreasi_Fermentech is above 86%, and the fulfilment of electricity needs by the Batutegi Turbine and Sekampung Turbine is above 97%. The calibration process of the Water Allocation Balance Model in the Sekampung System Irrigation within RIBASIM (1980-2023 period) used a discharge monitoring technique that compared the reliable discharge with the demand in the Sekampung System and Jabung irrigation districts, with the following results (see Figures 53 and 54):

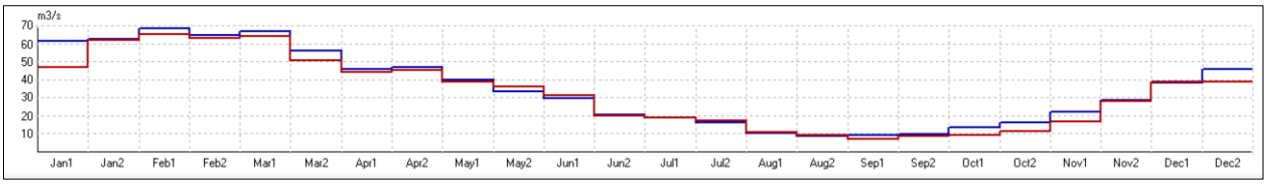

Figure 53. Comparison of dependable flow and pattern discharge for water demand in the Sekampung irrigation area

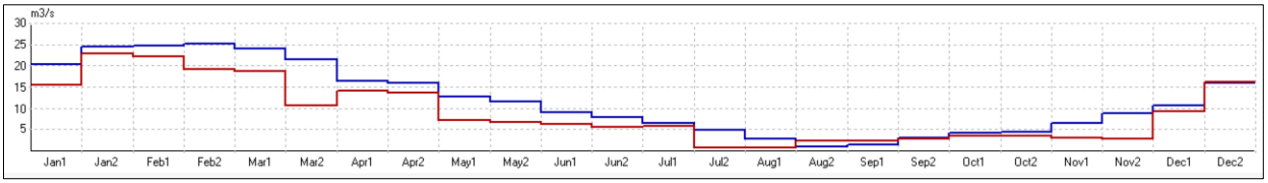

Figure 54. Comparison of dependable flow and pattern discharge for water demand in the Jabung irrigation area

4.4.9. Projected Response of Optimal Reservoir Operation Related to Climate Change

The water allocation balance was calculated based on the assumption that the period from 1980 to 2023 represents the existing conditions, i.e., the optimal reservoir operation pattern and infrastructure, as well as the existing supply and demand patterns will remain unchanged until 2023 (2023 Natural Resources Development Pattern, BBWS Mesuji – Sekampung). Climate projections for the period 2024–2100 were generated using 20 models (five climate change models with four scenarios), as described above. The optimal reservoir operation pattern, dam infrastructure operation, RKI demand withdrawal, and supply-demand pattern are assumed to remain unchanged from the existing conditions until 2023. Subsequently, an analysis of the water management system response at the Batutegi Cascade Dam System in meeting irrigation, DMI, and electricity production needs is conducted.

4.4.10. Water Allocation Balance Sheet Projections

Each discharge projection was then simulated in RIBASIM using the existing 2023 pattern. Twenty climate change models (described above in the previous subchapter) were used to examine the effects of climate change on projected rainfall patterns for the period 2024–2100. These projected rainfall patterns were then transformed using HEC-HMS to generate projected discharge for the period 2024–2100. The results are presented in Table 12.

Table 12. Percentage of water and energy supply affected by climate change

No.	CMIP 6 Model	Percentage of water Supply Fulfilment					Percentage of energy Fulfilment	
		Way Sekampung Irrigation Area (99%)	Jabung Irrigation Area (100%)	Pringsewu DMI (100%)	Lampung-Metro DMI (86%)	Tirta Kreasi DMI (100%)	Batutegi Reservoir Turbine (%)	Sekampung Reservoir Turbine (100%)
1	CanESM5_SSP126	99.4	99.4	100.0	97.9	100.0	97.3	100.0
2	CanESM5_SSP245	99.7	99.8	100.0	97.6	100.0	96.8	100.0
3	CanESM5_SSP370	99.0	98.2	100.0	97.3	99.9	96.3	100.0
4	CanESM5_SSP585	96.2	96.6	100.0	91.6	100.0	97.1	100.0
5	CESM2_SSP126	99.4	99.4	100.0	97.9	100.0	97.3	100.0
6	CESM2_SSP370	99.0	98.2	100.0	97.3	99.9	96.3	100.0
7	CESM2_SSP585	98.5	98.6	100.0	96.0	100.0	98.1	100.0
8	CESM2_SSP245	99.2	99.1	100.0	97.6	100.0	97.3	100.0
9	Micro6_SSP126	100.0	100.0	100.0	99.9	100.0	99.6	100.0
10	Micro6_SSP245	100.0	100.0	100.0	100.0	100.0	100.0	100.0
11	Micro6_SSP370	96.4	95.3	100.0	95.9	99.5	93.1	99.9
12	Micro6_SSP585	100.0	100.0	100.0	99.9	100.0	99.2	100.0
13	MPI2HR_SSP126	99.8	100.0	100.0	99.7	100.0	98.1	100.0
14	MPI2HR_SSP245	99.1	98.8	100.0	98.8	100.0	97.7	100.0
15	MPI2HR_SSP370	100.0	100.0	100.0	100.0	100.0	100.0	100.0
16	MPI2HR_SSP585	99.8	99.3	100.0	99.2	100.0	99.6	100.0
17	MPI2LR_SSP126	100.0	100.0	100.0	100.0	100.0	97.1	100.0
18	MPI2LR_SSP245	100.0	100.0	100.0	99.9	100.0	96.8	100.0
19	MPI2LR_SSP370	100.0	100.0	100.0	99.9	100.0	99.1	100.0
20	MPI2LR_SSP585	100.0	100.0	100.0	100.0	100.0	97.0	100.0

When grouped based on a comparison of existing conditions in 2023, it can be illustrated graphically as shown in the pie chart below (Figure 55):

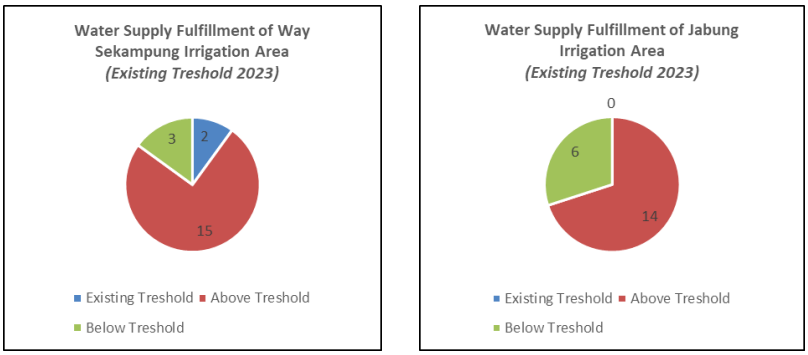

Figure 55. Water Supply Diagram

Based on the results of the analysis shown graphically in Figure 55, it can be concluded that for water supply at the Argoguruh Dam (DI. Sekampung System), 15 climate change models are above the threshold when compared to existing conditions, 3 climate change models are below the existing threshold, and 2 models are the same as existing conditions. For the water supply at the Jabung Weir (Jabung IA), 14 climate change models exceed the existing threshold, and 6 models fall below it (Figure 56).

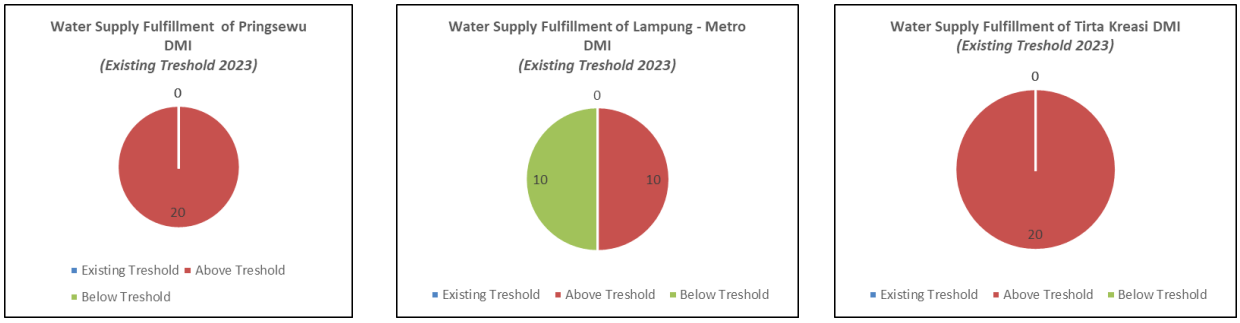

Figure 56. Water supply diagram for the Jabung Irrigation Area

Based on the results of the graphical analysis shown in Figure 56, it can be concluded that, in terms of water supply for DMI Pringsewu and DMI Tirta Kreasi, almost all models (20 climate change models) exceed the threshold when compared to existing conditions. Water supply for DMI Lampung Metro: 10 climate change models exceed the existing threshold, and 10 models fall below it (Figure 57).

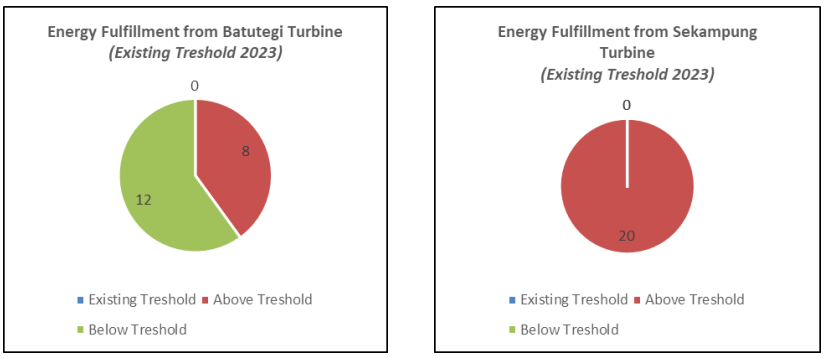

Figure 57. Existing threshold energy supply

Based on the results of the analysis displayed graphically in Figure 57, it can be concluded that for the fulfilment of hydroelectric power for the Batutegi 12 turbine, 12 climate change models are below the existing threshold, and 8 models are above it. Fulfilment of hydroelectric power for the Way Sekampung turbine dam. All models (20 climate change models) are above the threshold when compared to existing conditions.

5. Conclusion

The results show that the CMIP6 projection model accurately represents rainfall characteristics in the Way Sekampung River Basin during the periods of January–February and May–July. However, the accuracy of the model decreases in March and April, as well as in October and November. Most models tend to overestimate annual rainfall compared to observational data, but they are better at representing low rainfall amounts. This is important because low discharge is a critical consideration in calculating water availability for reservoir operations.

River discharge fluctuations follow rainfall variability, especially during the dry season. Daily discharge modeling shows significant changes in reliable discharge, especially in the Q10% to Q100% range. Despite the increasing rainfall trend, the 2023 reservoir operation pattern remains able to meet water demand, although a potential deficit persists during certain critical periods.

Synthetic discharge from rainfall-runoff modeling has been calibrated using observed discharge data. This modeling is used to estimate changes in flow discharge resulting from climate change, based on rainfall projections from various climate models and scenarios up to 2100. Several models predict a significant increase in local discharge, particularly for high-discharge events at the Argoguruh Dam, Margatiga Dam, and Jabung Dam. This analysis does not aim to determine the best climate model, but rather to adjust the discharge data produced to the relevant model conditions and climate scenarios at the study site.

The optimization modeling results indicate the need for adaptive and responsive reservoir operation rules to climate scenario changes so that the success rate of meeting multisectoral water needs reaches 80%. Several water management objectives, such as flood control and conservation, are projected to not be fully achieved by the end of this century. Almost all climate-rainfall-discharge models respond with discharge values above the range of the 1980–2023 hydrological year. In general, the 2024–2100 hydrological period is projected to be wetter than the historical period of 1980–2023.

This confirms that climate change is occurring in the Sekampung River Basin and that infrastructure managers and their operational patterns must adapt to these changes. These findings also underscore the importance of integrating climate models into watershed-based water resource management planning to enhance resilience to extreme events.

6. Declarations

6.1. Author Contributions

Conceptualization, A.L.; methodology, R.T.L.; software, A.F.; validation, F.M.; formal analysis, R.K.; investigation, F.L.; writing—original draft preparation, M.R.; writing—review and editing, W.L. All authors have read and agreed to the published version of the manuscript.

6.2. Data Availability Statement

The data presented in this study are available on request from the corresponding author.

6.3. Funding

The authors received no financial support for the research, authorship, and/or publication of this article.

6.4. Acknowledgements

Thank you to Hasanuddin University, the Mesuji Sekampung River Basin Authority, the Directorate General of Water Resources of the Ministry of Public Works, the Human Resources Development Agency of the Ministry of Public Works, and the team (Ms. Dian Indrawati, Mr. Firdaus Larossa, Mr. Asep Ferdiansyah, Mr. Mirwan Rofiq Ginanjar, and Mr. Widi Lesmana), as well as my family, my wife Maria Santisima Gama, and my seven children, who have made significant contributions to the implementation of this research.

6.5. Conflicts of Interest

The authors declare no conflict of interest.

7. References

[1] IPCC. (2021). Climate change 2021: The physical science basis. Contribution of Working Group I to the Sixth Assessment Report of the Intergovernmental Panel on Climate Change. Cambridge University Press, Cambridge, United Kingdom. Available online https://www.ipcc.ch/report/ar6/wg1/ (accessed on September 2025).

[2] Song, F., Leung, L. R., Lu, J., Zhou, T., & Huang, P. (2023). Advances in understanding the changes of tropical rainfall annual cycle: a review. Environmental Research: Climate, 2(4), 42001. doi:10.1088/2752-5295/acf606.

[3] Song, F., Dong, H., Wu, L., Leung, L. R., Lu, J., Dong, L., Wu, P., & Zhou, T. (2025). Hot season gets hotter due to rainfall delay over tropical land in a warming climate. Nature Communications, 16(1), 2188. doi:10.1038/s41467-025-57501-6.

[4] Ktavina, V. (2021). Way Sekampung and the future of Lampung farmers. Kompas, Jakarta, Indonesia. Available online: https://www.kompas.id/artikel/way-sekampung-dan-masa-depan-petani-lampung (accessed on September 2025). (In Malay).

[5] Yang, J., Cheng, C., Wang, Z., & Liu, P. (2024). Projected dryness/wetness pattern and influence factors in China under the CMIP6 scenarios for 2021–2100. Geomatics, Natural Hazards and Risk, 15(1), 2415529. doi:10.1080/19475705.2024.2415529.

[6] Almazroui, M., Islam, M. N., Saeed, F., Saeed, S., Ismail, M., Ehsan, M. A., Diallo, I., O'Brien, E., Ashfaq, M., Martínez-Castro, D., Cavazos, T., Cerezo-Mota, R., Tippett, M. K., Gutowski, W. J., Alfaro, E. J., Hidalgo, H. G., Vichot-Llano, A., Campbell, J. D., Kamil, S., … Barlow, M. (2021). Projected Changes in Temperature and Precipitation Over the United States, Central America, and the Caribbean in CMIP6 GCMs. Earth Systems and Environment, 5(1), 1–24. doi:10.1007/s41748-021-00199-5.

[7] Ge, F., Zhu, S., Peng, T., Zhao, Y., Sielmann, F., Fraedrich, K., Zhi, X., Liu, X., Tang, W., & Ji, L. (2019). Risks of precipitation extremes over Southeast Asia: Does 1.5°c or 2°c global warming make a difference? Environmental Research Letters, 14(4), 44015. doi:10.1088/1748-9326/aaff7e.

[8] Rizaldi, A., Darmawan, A., Kaskoyo, H., & Mubarok, H. (2021). dentification of Land Cover Changes as a Basis for Forest Management Strategies (Case Study of the Batutegi Protected Forest Management Unit, Lampung). Prosiding Fahutan, 2(02). (In Indonesian).

[9] Hijioka, Y., Lin, E., Pereira, J. J., Corlett, R. T., Cui, X., Insarov, G., ... & Wang, W. (2014). IPCC Fifth Assessment Report: Chapter 24 Asia. Climate Change 2014-Impacts, Adaptation and Vulnerability: Part B: Regional Aspects Working Group II Contribution to the IPCC Fifth Assessment Report, 1327-1370.

[10] Riahi, K., van Vuuren, D. P., Kriegler, E., Edmonds, J., O'Neill, B. C., Fujimori, S., Bauer, N., Calvin, K., Dellink, R., Fricko, O., Lutz, W., Popp, A., Cuaresma, J. C., KC, S., Leimbach, M., Jiang, L., Kram, T., Rao, S., Emmerling, J., … Tavoni, M. (2017). The Shared Socioeconomic Pathways and their energy, land use, and greenhouse gas emissions implications: An overview. Global Environmental Change, 42, 153–168. doi:10.1016/j.gloenvcha.2016.05.009.

[11] Bauer, N., Calvin, K., Emmerling, J., Fricko, O., Fujimori, S., Hilaire, J., Eom, J., Krey, V., Kriegler, E., Mouratiadou, I., Sytze de Boer, H., van den Berg, M., Carrara, S., Daioglou, V., Drouet, L., Edmonds, J. E., Gernaat, D., Havlik, P., Johnson, N., … van Vuuren, D. P. (2017). Shared Socio-Economic Pathways of the Energy Sector – Quantifying the Narratives. Global Environmental Change, 42, 316–330. doi:10.1016/j.gloenvcha.2016.07.006.

[12] Shindell, D. T., Lamarque, J. F., Schulz, M., Flanner, M., Jiao, C., Chin, M., Young, P. J., Lee, Y. H., Rotstayn, L., Mahowald, N., Milly, G., Faluvegi, G., Balkanski, Y., Collins, W. J., Conley, A. J., Dalsoren, S., Easter, R., Ghan, S., Horowitz, L., … Lo, F. (2013). Radiative forcing in the ACCMIP historical and future climate simulations. Atmospheric Chemistry and Physics, 13(6), 2939–2974. doi:10.5194/acp-13-2939-2013.

[13] Larsen, D., Bursi, J., Waldron, B., Schoefernacker, S., & Eason, J. (2020). Recharge pathways and rates for a sand aquifer beneath a loess-mantled landscape in western Tennessee, USA. Journal of Hydrology: Regional Studies, 28, 100667. doi:10.1016/j.ejrh.2020.100667.

[14] Kundzewicz, Z. W., Krysanova, V., Dankers, R., Hirabayashi, Y., Kanae, S., Hattermann, F. F., Huang, S., Milly, P. C. D., Stoffel, M., Driessen, P. P. J., Matczak, P., Quevauviller, P., & Schellnhuber, H.-J. (2016). Differences in flood hazard projections in Europe – their causes and consequences for decision making. Hydrological Sciences Journal, 1241398. doi:10.1080/02626667.2016.1241398.

[15] USAE-HEC-HMS. (2000). Hydrologic Modeling System Technical Reference Manual. In Hydrologic Modeling System HEC-HMS Technical Reference Manual (Issue March). US Army Corps of Engineers, Hydrologic Engineering Center, New Jersey, United States.

[16] Arnold, J. G., Moriasi, D. N., Gassman, P. W., Abbaspour, K. C., White, M. J., Srinivasan, R., ... & Jha, M. K. (2012). SWAT: Model use, calibration, and validation. Transactions of the ASABE, 55(4), 1491-1508. doi:10.13031/2013.42256.

[17] oucks, D. P., & van Beek, E. (2017). Water Resource Systems Planning and Management. Springer International Publishing, Cham, Switzerland. doi:10.1007/978-3-319-44234-1.

[18] Ahmadzadeh, H., Jamali, A., & Karamouz, M. (n.d.). River basin simulation modeling for integrated water resources planning. Environmental Modeling & Assessment, 27(1), 75–92. doi:10.1007/s10666-021-09787-0.

[19] Patil, J. P., Gurjar, S., Bons, C. A., & Goel, M. K. (2021). Strategic Analysis of Water Resources in the Ganga Basin, India. The Ganga River Basin: A Hydrometeorological Approach, 309-322. doi:10.1007/978-3-030-60869-9_20.

[20] Klein Tank, A. M. G., Zwiers, F. W. & Zhang, X. B. (2009). Guidelines on analysis of extremes in a changing climate in support of informed decisions for adaptation. WCDMP No. 72, World Meteorological Organization, Geneva, Switzerland.

[21] Moriasi, D. N., Arnold, J. G., Van Liew, M. W., Bingner, R. L., Harmel, R. D., & Veith, T. L. (2007). Model evaluation guidelines for systematic quantification of accuracy in watershed simulations. Transactions of the ASABE, 50(3), 885-900. doi:10.13031/2013.23153.

[22] Cabrera, J. (2012). Calibration of hydrological models. Instituto para la Mitigación de los Efectos del Fenómeno El Niño, Universidad Nacional de Ingeniería, Facultad de Ingeniería Civil, Perú, 1(1). (In Spanish).

[23] Zuo, J., Pullen, S., Palmer, J., Bennetts, H., Chileshe, N., & Ma, T. (2015). Impacts of heat waves and corresponding measures: a review. Journal of Cleaner Production, 92, 1–12. doi:10.1016/j.jclepro.2014.12.078.

[24] Cook, M. A., King, C. W., Davidson, F. T., & Webber, M. E. (2015). Assessing the impacts of droughts and heat waves at thermoelectric power plants in the United States using integrated regression, thermodynamic, and climate models. Energy Reports, 1, 193–203. doi:10.1016/j.egyr.2015.10.002.

[25] Ehsani, N., Vörösmarty, C. J., Fekete, B. M., & Stakhiv, E. Z. (2017). Reservoir operations under climate change: Storage capacity options to mitigate risk. Journal of Hydrology, 555, 435–446. doi:10.1016/j.jhydrol.2017.09.008.

[26] Hulme, M. & Sheard, N. (1999). Climate Change Scenarios for Indonesia. Climatic Research Unit, Norwich, United Kingdom.

[27] Boer, R., & Faqih, A. (2004). Current and future rainfall variability in Indonesia. An Integrated Assessment of Climate Change Impacts, Adaptation and Vulnerability in Watershed Areas and Communities in Southeast Asia, Report from AIACC Project No AS21, Int. START Secretariat, Washington, United States.

[28] Case, M., Ardiansyah, F., & Spector, E. (2007). Climate change in Indonesia. South-East Asia's environmental future: the search for sustainability. WWF-International Climate Change Programme, 1-15.

[29] Karaeren, V. (2014). Maximizing energy generation of a cascade hydropower system. Master Thesis, Middle East Technical University, Ankara, Türkiye.

[30] Sadollah, A., Nasir, M., & Geem, Z. W. (2020). Sustainability and Optimization: From Conceptual Fundamentals to Applications. Sustainability, 12(5), 2027. doi:10.3390/su12052027.

[31] Eyring, V., Bony, S., Meehl, G. A., Senior, C. A., Stevens, B., Stouffer, R. J., & Taylor, K. E. (2016). Overview of the Coupled Model Intercomparison Project Phase 6 (CMIP6) experimental design and organization. Geoscientific Model Development, 9(5), 1937–1958. doi:10.5194/gmd-9-1937-2016.

[32] Das, P., & Ganguly, A. R. (2025). Finer resolutions and targeted process representations in earth system models improve hydrologic projections and hydroclimate impacts. NPJ Climate and Atmospheric Science, 8(1), 247. doi:10.1038/s41612-025-01134-5.

[33] Thrasher, B., Khajehei, S., Kim, J. B., & Brosnan, I. (2024). NASA Earth Exchange Downscaled Climate Projections 30 Arcseconds CMIP6. Scientific Data, 11(1), 1346. doi:10.1038/s41597-024-04188-x.

[34] Wikipedia. (2025). Köppen climate classification (Klasifikasi iklim Köppen). Wikipedia. Available online: https://id.wikipedia.org/wiki/Klasifikasi_iklim_K%C3%B6ppen (accessed September 2025).

[35] USACE. (2008) Hydrologic Modeling System HEC-HMS. User's Manual. Hydrologic Engineering Center, Washington, United States.

[36] Swastika, D., Wulandari, D. A., & Sriyana, I. (2023). Simulation of Batutegi Reservoir Operation Pattern, Lampung Province. Cantilever: Jurnal Penelitian Dan Kajian Bidang Teknik Sipil, 11(2), 81-92. doi:10.35139/cantilever.v11i2.149.

[37] Balai Besar Wilayah Sungai (BBWS) Mesuji–Sekampung. (2023). Technical documentation and data on water resource management patterns in the Sekampung River Basin. Kementerian Pekerjaan Umum dan Perumahan Rakyat, Jakarta, Indonesia. (In Indonesian).

[38] Al Hamid, I. M. I. (2024). Operation Optimization of Batujai Cascade Reservoir and Pengga Using HEC-ResSim Software. Ph.D. Thesis, Universitas Gadjah Mada, Yogyakarta, Indonesia. (In Indonesian).

[39] Chen, S., Xu, Y. P., Guo, Y., & Yu, X. (2025). Multi-objective optimization of urban water allocation considering recycled water. Water Resources Management, 39(6), 2615-2631. doi:10.1007/s11269-024-04081-7.

[40] Tang, R., & Wang, Y. (2025). Risk-Informed Multiobjective Optimization of Reservoir Operation. Water (Switzerland), 17(16), 2467. doi:10.3390/w17162467.

[41] Getahun, E., Prada, A. F., Zhang, Z., Keefer, L., & Qie, G. (2025). Comprehensive Hydrologic Modeling for Evaluating Impacts of Future Water Uses and Climate Change on Water Resources Sustainability. Water Resources Management. doi:10.1007/s11269-025-04333-0.

[42] Lee, E., Ji, J., Yi, S., Lee, S., Yoon, J., & Yi, J. (2025). Developing Resilient Reservoir System Operations: A Simulation Approach Incorporating Rule Curve. Water Resources Management, 39(13), 6889–6905. doi:10.1007/s11269-025-04280-w.